

2083883CD1_PRT_2_PF-0721-USN

739 aa

ACSL5

739 aa

Fatty-acid-Coenzyme A ligase long-chain 5 (acyl-CoA synthetase 5), catalyzes the synthesis of acyl-CoA from fatty acids, ATP and CoA, plays a role in cell growth, upregulated in glioblastomas and grade IV primary gliomas

Match: Length=739, Identity: 99%, Similarity:100%, Query Overlap: 100%, Subject Overlap: 100%, E-value:0.0, Score:1501

```

Query: 1 MDALKPPCLWRNHERGKKDRDSCGRKNSEPGSPHSLEALRDAAPSQGLNFLLFTKMLFI 60
       MDALKPPCLWRNHERGKKDRDSCGRKNSEPGSPHSLEALRDAAPSQGLNFLLFTKMLFI
Sbjct: 1 MDALKPPCLWRNHERGKKDRDSCGRKNSEPGSPHSLEALRDAAPSQGLNFLLFTKMLFI 60

Query: 61 FNFLFSPLPTPALICILTFGAAIFLWLITRPQPVLPLLDLNNSQVGIEGGARKGVSQKNN 120
       FNFLFSPLPTPALICILTFGAAIFLWLITRPQPVLPLLDLNNSQVGIEGGARKGVSQKNN
Sbjct: 61 FNFLFSPLPTPALICILTFGAAIFLWLITRPQPVLPLLDLNNSQVGIEGGARKGVSQKNN 120

Query: 121 DLTSCCFSDAKTMYEVFQRGLAVSDNGPCLGYRKPNQPYRWLSYKVSDRAEYLGSCLLH 180
       DLTSCCFSDAKTMYEVFQRGLAVSDNGPCLGYRKPNQPYRWLSYKVSDRAEYLGSCLLH
Sbjct: 121 DLTSCCFSDAKTMYEVFQRGLAVSDNGPCLGYRKPNQPYRWLSYKVSDRAEYLGSCLLH 180

Query: 181 KGYKSSPDQFVGIFAQNRPWEIISELACYTYSMVAVPLYDTLGPEAIVHIVNKADIAVI 240
       KGYKSSPDQFVGIFAQNRPWEIISELACYTYSMVAVPLYDTLGPEAIVHIVNKADIA+VI
Sbjct: 181 KGYKSSPDQFVGIFAQNRPWEIISELACYTYSMVAVPLYDTLGPEAIVHIVNKADIAMVI 240

Query: 241 CDTPQKALVLIGNVEKGFTPSLKVIILMDPFDDDLKQRGEKSGIEILSLYDAENLGKEHF 300
       CDTPQKALVLIGNVEKGFTPSLKVIILMDPFDDDLKQRGEKSGIEILSLYDAENLGKEHF
Sbjct: 241 CDTPQKALVLIGNVEKGFTPSLKVIILMDPFDDDLKQRGEKSGIEILSLYDAENLGKEHF 300

Query: 301 RKPVPPSPEDLSVICFTSGTTGDPKGAMITHQNIVSNAAFLKCVEHAYEPTPDDVAISY 360
       RKPVPPSPEDLSVICFTSGTTGDPKGAMITHQNIVSNAAFLKCVEHAYEPTPDDVAISY
Sbjct: 301 RKPVPPSPEDLSVICFTSGTTGDPKGAMITHQNIVSNAAFLKCVEHAYEPTPDDVAISY 360

Query: 361 LPLAHMFERIVQAVVYSCGARVGFFQGDIRLLADDMKTLPKTLFPAPVPRLLNRIYDKVQN 420
       LPLAHMFERIVQAVVYSCGARVGFFQGDIRLLADDMKTLPKTLFPAPVPRLLNRIYDKVQN
Sbjct: 361 LPLAHMFERIVQAVVYSCGARVGFFQGDIRLLADDMKTLPKTLFPAPVPRLLNRIYDKVQN 420

Query: 421 EAKTPLKKFLLKLAVSSKFKELOKGIIRHDSFWDKLIFAKIQDSLGGRVRVIVTGAAPMS 480
       EAKTPLKKFLLKLAVSSKFKELOKGIIRHDSFWDKLIFAKIQDSLGGRVRVIVTGAAPMS
Sbjct: 421 EAKTPLKKFLLKLAVSSKFKELOKGIIRHDSFWDKLIFAKIQDSLGGRVRVIVTGAAPMS 480

Query: 481 TSVMTFFRAAMGCQVYEAYGQTECTGGCTFTLPGDWTSGHGVGVPLACNYVKLEDVADMNY 540
       TSVMTFFRAAMGCQVYEAYGQTECTGGCTFTLPGDWTSGHGVGVPLACNYVKLEDVADMNY
Sbjct: 481 TSVMTFFRAAMGCQVYEAYGQTECTGGCTFTLPGDWTSGHGVGVPLACNYVKLEDVADMNY 540

Query: 541 FTVNNEGEVCIKGTNVFKGYLKDPKETQEALDSGWLHTGDIGRWLPGNTLKIIDRKKNI 600
       FTVNNEGEVCIKGTNVFKGYLKDPKETQEALDSGWLHTGDIGRWLPGNTLKIIDRKKNI
Sbjct: 541 FTVNNEGEVCIKGTNVFKGYLKDPKETQEALDSGWLHTGDIGRWLPGNTLKIIDRKKNI 600

Query: 601 FKLAQGEYIAPEKIEINIYNRSQPVLIQIFVHGESLRSSLGVVVVPDTDVLPSFAAKLGVKG 660
       FKLAQGEYIAPEKIEINIYNRSQPVLIQIFVHGESLRSSLGVVVVPDTDVLPSFAAKLGVKG

```

BEST AVAILABLE COPY

Alignment

Sbjct: 601 FKLAQGEYIAPEKIEINIYNRSQPVLQIFVHGESLRSSLGVVVVPDTDVLPSFAAKLGVKG 660

Query: 661 SFEELCQNQVVREAILEDLQKIGKESGLKTFEQVKAIFLHPEPFSIENLLPTLKAKRG 720
SFEELCQNQVVREAILEDLQKIGKESGLKTFEQVKAIFLHPEPFSIENLLPTLKAKRG

Sbjct: 661 SFEELCQNQVVREAILEDLQKIGKESGLKTFEQVKAIFLHPEPFSIENLLPTLKAKRG 720

Query: 721 ELSKYFRTQIDSLYEHIQD 739

ELSKYFRTQIDSLYEHIQD

Sbjct: 721 ELSKYFRTQIDSLYEHIQD 739

Schematic Colors:

Very Strong	Strong	High	Moderate	Low	Weak
>95%	80-95%	45-80%	35-45%	25-35%	20-25%

Fatty acid induced glioma cell growth is mediated by the acyl-CoA synthetase 5 gene located on chromosome 10q25.1-q25.2, a region frequently deleted in malignant gliomas

Y.C. Yamashita^{1,2}, Toshihiro Kumabe², Yong-Yeon Cho¹, Mika Watanabe³, Jun Kawagishi², Takashi Yoshimoto², Takahiro Fujino¹, Man-Jong Kang¹ and Tokuo T Yamamoto^{*1}

¹Tohoku University Gene Research Center, Sendai 981-8555, Japan; ²Department of Neurosurgery, Tohoku University School of Medicine, Sendai 980-8574, Japan; ³Department of Pathology, Tohoku University School of Medicine, Sendai 980-8574, Japan

Acyl-CoA synthetase (ACS) ligates fatty acid and CoA to produce acyl-CoA, an essential molecule in fatty acid metabolism and cell proliferation. ACS5 is a recently characterized ACS isozyme highly expressed in proliferating 3T3-L1 cells. Molecular characterization of the human ACS5 gene revealed that the gene is located on chromosome 10q25.1-q25.2, spans approximately 46 kb, comprises 21 exons and 22 introns, and encodes a 683 amino acid protein. Two major ACS5 transcripts of 2.5- and 3.7-kb are distributed in a wide range of tissues with the highest expression in uterus and spleen. Markedly increased levels of ACS5 transcripts were detected in a glioma line, A172 cells, and primary gliomas of grade IV malignancy, while ACS5 expression was found to be low in normal brain. Immunohistochemical analysis also revealed strong immunostaining with an anti-ACSS antibody in glioblastomas. U87MG glioma cells infected with an adenovirus encoding ACS5 displayed induced cell growth on exposure to palmitate. Consistent with the induction of cell growth, the virus infected cells displayed increased uptake of palmitate. These results demonstrate a novel fatty acid-induced glioma cell growth mediated by ACS5. *Oncogene* (2000) 19, 5919–5925.

Keywords: acyl-CoA synthetase; fatty acid; glioma; growth stimulation

Introduction

Acyl-CoA synthetase (ACS, EC6.2.1.3) catalyzes the formation of acyl-CoA from fatty acid, ATP and CoA. This reaction is essential in mammalian fatty acid metabolism, including the catabolic pathway for the degradation of fatty acid via the β -oxidation system and the anabolic pathway for the synthesis of cellular lipids. ACS also plays a role in cell proliferation by providing acyl-CoAs for the synthesis of membrane phospholipids. Tomoda *et al.* (1991) have shown that specific inhibitors of ACS, triacins, profoundly reduce the synthesis of cellular phospholipids, and that this blockade of acyl-CoA synthesis results in the inhibition of cell proliferation.

In addition to fatty acid metabolism, ACS mediates the transportation of fatty acids into cells by

cooperating with fatty acid transporter (Schaffer and Lodish, 1994). By expression cloning, Schaffer and Lodish identified two proteins that promote uptake of long chain fatty acid into 3T3-L1 cells: one is an integral plasma membrane protein of 63 kDa, termed fatty acid transport protein; which later turned out to be identical to very long chain acyl-CoA synthetase (Coe *et al.*, 1999); and the other is identical to ACS1 (Suzuki *et al.*, 1990). These studies suggest that ACS facilitates the uptake of long chain fatty acid into cells. Furthermore, recent studies by Yagasaki *et al.* (1999) have identified the human ACS2 gene as a new *ets* variant gene 6 (ETV6) fusion partner in a patient with refractory anemia with excess blasts with basophilia, a patient with acute myelogenous leukemia with eosinophilia and a patient with acute eosinophilic leukemia. The ETV6/ACS2 fusion in these patients disrupts both the ACS2 and ETV6 genes, suggesting that ACS2 is also involved in the pathogenesis of hematologic malignancies.

In previous studies, we have characterized five ACSs (Fujino *et al.*, 1996; Fujino and Yamamoto, 1992; Kang *et al.*, 1997; Oikawa *et al.*, 1998; Suzuki *et al.*, 1990) that show different levels of expression in different tissues. ACS1, ACS2 and ACS5 are structurally similar enzymes that exhibit similar broad fatty acid preferences. Of these three enzymes, ACS5 is most abundant in intestinal epithelial cells, and is also highly expressed in undifferentiated proliferating 3T3-L1 preadipocytes (Oikawa *et al.*, 1998). Since ACS1 and ACS2 are almost undetectable in proliferating 3T3-L1 preadipocytes, ACS5 may provide the acyl-CoA required for the synthesis of cellular lipids during cell proliferation (Oikawa *et al.*, 1998).

During characterization of the human ACS5 gene and transcripts, we found that: (i) the gene is located on chromosome 10q25.1-q25.2, a region frequently deleted in malignant gliomas (Bergerheim *et al.*, 1991; Herbst *et al.*, 1994; Karlstrom *et al.*, 1993; Peiffer *et al.*, 1995; Rasheed *et al.*, 1992, 1995); and (ii) the levels of ACS5 mRNA are markedly increased in primary glioblastomas. Here we provide evidence that ACS5 mediates glioma cell growth by facilitating fatty acid transportation into cells.

Results

Molecular characterization of the human ACS5 gene

As an initial approach to evaluate the role of ACS5, we first characterized the human ACS5 gene. A near full-

*Correspondence: TT Yamamoto, Tohoku University Gene Research Center, 1-1 Tsutsumidori-Ainamiya, Aoba Sendai 981-8555, Japan

Received 27 June 2000; revised 26 September 2000; accepted 3 October 2000

length cDNA for human ACS5 was isolated from a human liver cDNA library using rat ACS5 cDNA (Oikawa *et al.*, 1998) as a probe, and was completely sequenced (GeneBank Accession No. AB033899). The insert of the human ACS5 cDNA contains 154 nucleotides in the 5'-untranslated region, a 2052-nucleotide open reading frame encoding a protein of 683 amino acids with a calculated molecular weight of 75 957 and 1012 nucleotides in the 3'-untranslated region (Figure 1a). Between human and rat ACS5, approximately 80% of the amino acids are identical. BLAST searches of the RHdb databases (<http://www.ebi.ac.uk/RHdb/>) using the human ACS5 sequence reveal that the 3'-untranslated region contains a specific STS marker, WI-12237, which had been mapped to the q25.1-q25.2 region of chromosome 10.

To define the genomic structure of the human ACS5 gene, we isolated and characterized two overlapping BAC clones [60(n16), 116(b1)] from a human BAC library (Genome Systems) and four YAC clones (816g5, 935g4, 950e11 and 962h2) from Mega YAC libraries (see Materials and methods). Characterization of these clones revealed that the gene overlaps with WI-12237, which has been placed approximately 0.5 cM telomeric of D10S1564 and spans approximately 46 kb, and encodes 21 exons (Figure 1b,c). The 5'-untranslated region is encoded by exon 1, and a

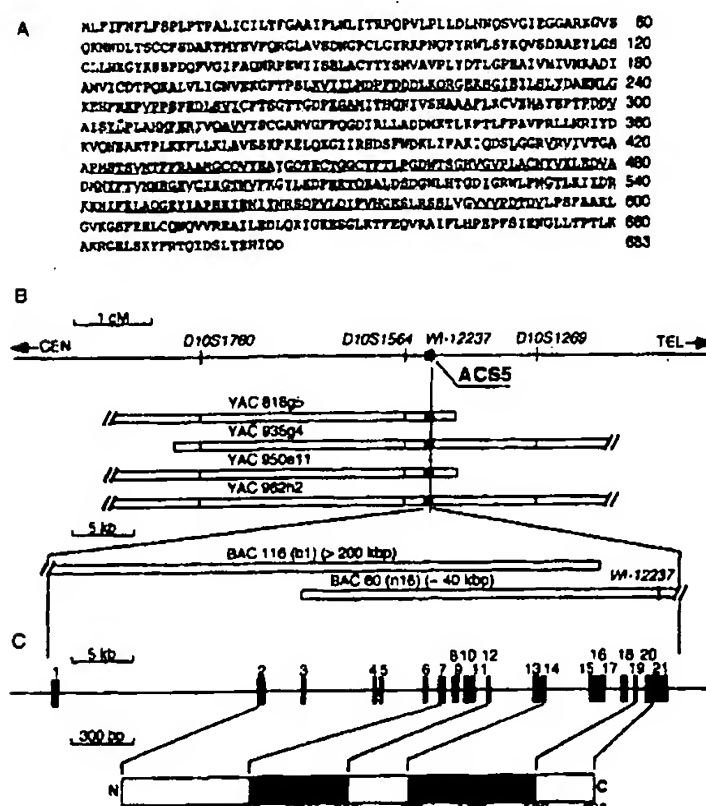


Figure 1 (a) Amino acid sequence of ACS5 deduced from the cDNA. Amino acids are numbered on the right. The two luciferase-like regions are underlined. (b) The YAC and BAC clones used for the analysis of the human ACS5 gene. Human chromosome 10q25.1-q25.2 region is represented schematically at the top of the diagram. CEN, centromere; TEL, telomere. The locations of STS markers are from the RHdb databases. (c) Diagram of the human ACS5 gene. Exons are indicated by numbers and closed boxes. ACS5 protein is schematically represented at the bottom of the diagram. LR1 and LR2: luciferase-like regions 1 and 2. The exon/intron boundary sequence information is available under GenBank Accession Nos. AB033900 to AB033920.

large intron of 15 kb separates it from exon 2, which contains the translation initiator codon AUG. Exon 21 contains the translation termination codon and the 3'-untranslated region. Functionally important luciferase-like regions (Suzuki *et al.*, 1990; Iijima *et al.*, 1996), LR1 and LR2, are encoded by exons 7–12 and exons 14–19, respectively. The relevant sequence information is available under GenBank Accession Nos. AB033900 to AB033920.

Expression of ACS5 in human tissues and gliomas

Northern blotting of multiple tissue blots with the human ACS5 probe revealed two major transcripts of 2.5 and 3.7 kb in a wide range of human tissues, with the highest levels in uterus and spleen; relatively high levels in liver, small intestine, colon, and peripheral blood leukocytes; and lower levels in heart, lung, thymus and prostate (Figure 2a). A trace amount of the mRNA was detected in brain, placenta, skeletal muscle, pancreas and kidney. In addition to the two transcripts with 2.5 and 3.7 kb, a unique transcript of 1.7 kb was detected only in testis. This major transcript in the testis may be a consequence of alternative splicing of pre-ACS5 mRNA, alternative transcription initiation of the ACS5 gene, degraded products of ACS5 mRNA, or an artifact of Northern blotting.

The location of the ACS5 gene, on chromosome region 10q25.1-25.2 region, is frequently deleted in malignant gliomas (Bergerheim *et al.*, 1991; Herbst *et al.*, 1994; Karlstrom *et al.*, 1993; Peiffer *et al.*, 1995; Rasheed *et al.*, 1992, 1995). Therefore, we analysed the levels of ACS5 transcripts in glioma cells and primary gliomas of various origins. Northern blotting of ACS5 transcripts in glioma cell lines A172, T98G, U251, U373MG and U87MG cells revealed an overproduction of ACS5 mRNA in A172 cells (Figure 2b) with levels approximately 40-fold higher than those in normal brains. RNAs from cases of human primary gliomas of malignancy grade ranging from II to IV according to the WHO criteria were also analysed (Figure 2c). As shown in Figure 2d, the levels of the mRNA were significantly higher in grade IV gliomas ($P < 0.05$, an average increase of 2.5-fold compared with normal brains). Furthermore, immunohistochemical analysis revealed significant immunostaining with an anti-ACS5 antibody in primary glioblastomas, while only a trace of immunoreactivity was detected in the normal cerebral white matter (Figure 3). We also analyzed the gene in patients with glioblastomas, however, there were no amplifications or rearrangements of the gene, except for a C to T substitution at nucleotide 111, which is also found in the normal populations.

Effects of ACS5 expression on cell growth and fatty acid uptake

To evaluate the effects of ACS5 expression on the growth of glioma cells, we constructed a recombinant adenovirus virus (designated AdAC5) containing the entire region of human ACS5 cDNA. U87MG cells, which showed the lowest expression of ACS5 mRNA among the five glioma cell lines tested, were infected with 5 moi of AdAC5 or control AdlacZ viruses. To minimize the effects of FCS on the growth of glioma

Figure 2 *in vitro* glioma cell expression indicated by hybridization of the figure RNA from glioma cell lines as described. The confluent typical autoradiograph is shown. Primary glioma cell loading with bromide solution (18 h exposure). Abundance was quantitated in each sample. The sample indicates $P < 0.05$.

cells, the FCS. In the reduced to presence of AdAC5, ACS5 protein growth in the presence of growth in

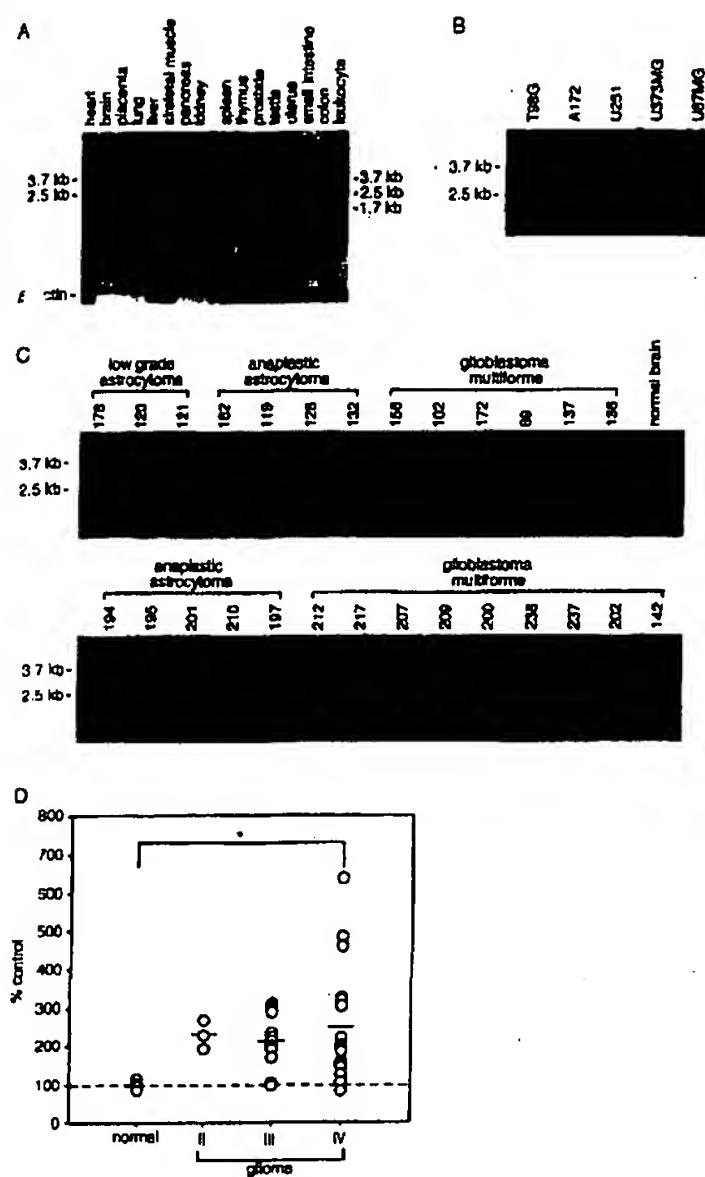


Figure 2 Expression of ACSS transcripts in human tissues, glioma cells and primary gliomas of various origin. (a) Tissue expression of ACSS transcripts. 2 µg of poly(A)⁺ RNA from the indicated human tissues was probed with [³²P]-labelled human ACSS cDNA. The filters were exposed to Kodak XAR-5 film with an intensifying screen at -80°C for 18 h. Control hybridization with a human β -actin probe is shown at the foot of the figure. (b) ACSS mRNA in glioma cell lines. 25 µg of total RNA from the indicated cells was analysed by Northern blotting as described previously. Volume of total RNA in each lane was confirmed by ethidium bromide staining (data not shown). A typical autoradiogram (18 h exposure) of triplicate hybridizations is shown. (c) Northern blotting of total RNA (25 µg) from primary gliomas of malignancy ranging from II-IV. RNA loading was consistent among lanes, as judged by ethidium bromide staining (data not shown). A typical autoradiogram (18 h exposure) of three independent hybridizations is shown. (d) Abundance of ACSS mRNAs in gliomas. Autoradiograms in (c) were quantified with a Bioimage Analyzer (BAS-2000, Fuji) and analysed statistically. The mean for normal brain (four different samples) is represented as 100 and abundance of ACSS mRNA in each sample was expressed as a percentage of this value. Bars indicate mean value of each grade. *Statistical difference at $P < 0.05$.

cells, the cells were cultured in the presence of 2% FCS. In this culture condition, the growth rate was reduced to approximately 30% of that cultured in the presence of 10% FCS. As shown in Figure 4a, AdACSS infected cells produced a large amount of ACSS protein after virus infection. Figures 4b,c show growth induction of AdACSS infected cells cultured in the presence of palmitate. Approximately 1.5–2.5-fold growth induction was observed in the presence of

30 µM palmitate, whereas almost no effects were observed on the growth of AdACSS infected cells cultured in the absence of palmitate or AdlacZ infected cells in the absence or the presence of palmitate. A modest but significant growth stimulation was also observed when uninfected A172 were exposed to 30 µM palmitate (data not shown). The maximal growth stimulation was observed at a palmitate concentration of 30 µM, the value close to the calculated K_d of the purified enzyme. However, at higher concentrations (>60 µM) palmitate was toxic to the cells. In the presence of 10% FCS, the fatty acid induced growth induction was not detected, presumably because the presence of free fatty acid bound to serum albumin. The conditioned medium of AdACSS infected U87MG cells exposed to palmitate had no growth stimulatory effects on uninfected cells (data not shown).

In the presence of palmitate, AdACSS infected cells tended to form multilayered foci at a subconfluent density, whereas AdlacZ infected cells grew as a flat monolayer (data not shown). Furthermore, DNA fragmentation analysis and TUNEL assay of glioma cells infected with AdACSS or AdlacZ did not show any evidence of apoptosis (data not shown).

Similar fatty acid induced cell growth was also seen in A172, T98G, U251 and U87MG glioma cells stably transfected with an ACSS expression plasmid (data not shown). In contrast to glioma cells, no growth stimulation was seen in Chinese hamster ovary, COS-6, HepG2, NIH3T3 or 3T3-L1 cells stably transfected with an ACSS expression plasmid (data not shown). These data indicate that fatty acid-induced cell growth mediated by ACSS is unique to glioma cells.

Regarding the specificity of fatty acid on the induction of glioma cell growth, Figure 4D shows that exposure of the AdACSS infected cells to myristate also induced cell growth, while essentially no effects were seen in the presence of oleate, linoleate or arachidonate.

To further define the mechanism of fatty acid induced glioma cell growth, we analysed the uptake of [¹⁴C]palmitate and -arachidonate by AdACSS infected cells. As shown in Figure 5, AdACSS infection increased [¹⁴C]palmitate uptake by approximately three-fold over the relatively low uptake by AdlacZ infected cells. In contrast, there were no differences in the uptake of [¹⁴C]arachidonate by AdACSS or AdlacZ infected cells.

Discussion

In the current studies, we have shown a novel growth induction of glioma cells mediated by ACSS. This growth induction may be of pathological significance for the development and progression of malignant gliomas.

The primary function of ACS is to produce acyl-CoA for numerous metabolic pathways including cellular lipid metabolism, transcriptional regulation (Henry and Cronan, 1992; Hertz *et al.*, 1998), intracellular protein transportation (Glick and Rothman, 1987), protein acylation (Grand, 1989) and protein kinase C mediated signal transduction (Bronfman *et al.*, 1989). A secondary function of ACS is that it facilitates fatty acid transportation into cells (Coe *et al.*,

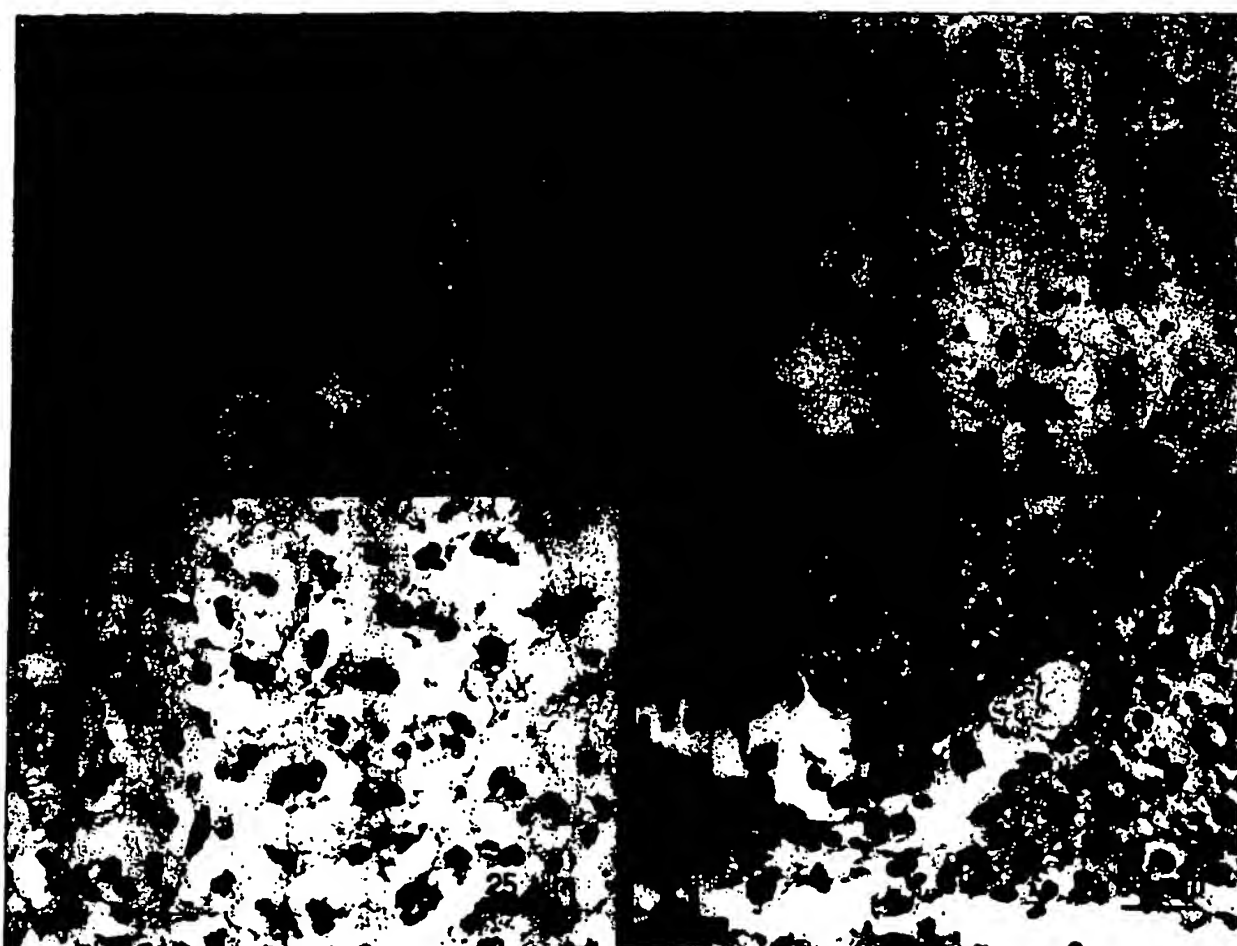


Figure 3 Immunostaining with anti-ACS. (a) Normal cerebral white matter and grade IV gliomas (case nos. 137, 172 and 217). Strong immunostaining is seen in neoplastic cells in all cases of grade IV gliomas. Bars: 25 μ m

al., 1999; Schaffer and Lodish, 1994). Consistent with the utilization of acyl-CoA in numerous metabolic pathways, there are multiple ACSs with distinct fatty acid specificities and different tissue distributions. Among the five known ACSs, ACS5 is believed to provide acyl-CoA for the synthesis of cellular lipid during cell proliferation. Consistent with our hypothesis, the levels of ACS5 transcripts and proteins are markedly increased in malignant gliomas.

Although the ACS5 gene is located on chromosome 10q25.1-25.2 region, there were no apparent gene rearrangements in the primary gliomas and the five glioma cell lines by Southern blotting. In contrast to the increment of ACS5 transcripts in primary glioblastomas, only a trace amount of the transcript was detected in glioma cell lines, T98G, U251, U373MG and U87MG. The sole exception was A172 cells, which exhibit 40-fold higher expression than those in the normal brain. This variation in glioma cell lines remains unknown.

U87MG cells infected with AdACS5 virus displayed induced cell growth by exposure to saturated fatty acids, palmitate and myristate, but not by unsaturated fatty acids including arachidonate and linolenate. This fatty acid induced cell growth mediated by ACS5 is unique to glioma cells (A172, T98G, U251 and U87MG cells), and was not observed in other cells, including Chinese hamster ovary, COS-6, HepG2, NIH3T3, or 3T3-L1 cells. Consistent with the induction of cell growth, U87MG cells infected with AdACS5 displayed induced uptake of palmitate, but did not show stimulation of arachidonate uptake, indicating that facilitated palmitate uptake may promote the induction of cell growth.

Although the mechanism(s) by which fatty acid induces glioma cell growth remain to be elucidated, there may be some relation with the intracellular fatty acid/acyl-CoA pool utilized for the synthesis of cellular lipids including membrane phospholipids. Pizer *et al.* (1998) have shown that inhibition of fatty acid synthase by its specific inhibitors, cerulenin and c75, results in the suppression of DNA replication and induces apoptosis in various tumor cell lines. Triacins block the supply of acyl-CoAs, mainly for lipid synthesis, and also subsequently causes inhibition of cell growth (Tomoda *et al.*, 1991). These growth suppression effects by fatty acid synthase and ACS inhibitors apparently relate to the tumor cell phenotype of abnormally elevated fatty acid metabolism (Kuhajda *et al.*, 1994; Tomoda *et al.*, 1991). The increased levels of ACS5 in malignant glioma may support the aggressive cell growth by increasing the size of the intracellular fatty acid/acyl-CoA pool.

In contrast to the increment of ACS5 in malignant gliomas, the ACS2 gene is disrupted by fusion of the ETV6 gene in myelodysplastic syndrome and acute myelogenous leukemia, suggesting that ACS2 acts as a tumor suppressor in hematopoietic cells (Yagasaki *et al.*, 1999). Together with our current data, it is suggested that the role of ACS5 in cell proliferation differs from that of ACS2. There may be a different fatty acid/acyl-CoA pool provided by ACS2 that may induce apoptosis in hematopoietic cells during differentiation. Although further studies are necessary to demonstrate the exact roles of ACSs in cell proliferation, our current data have clearly demonstrated that ACS5 mediates novel fatty acid-induced glioma cell growth.

Figure 4
infection
transferr.
course c
concentr.
AdACS5
2% FCS
2% FCS
percenta
growth. 1
virus inf.
cultured
mediated
with 1%
acids: 14

Figure 5
infection.
as descri

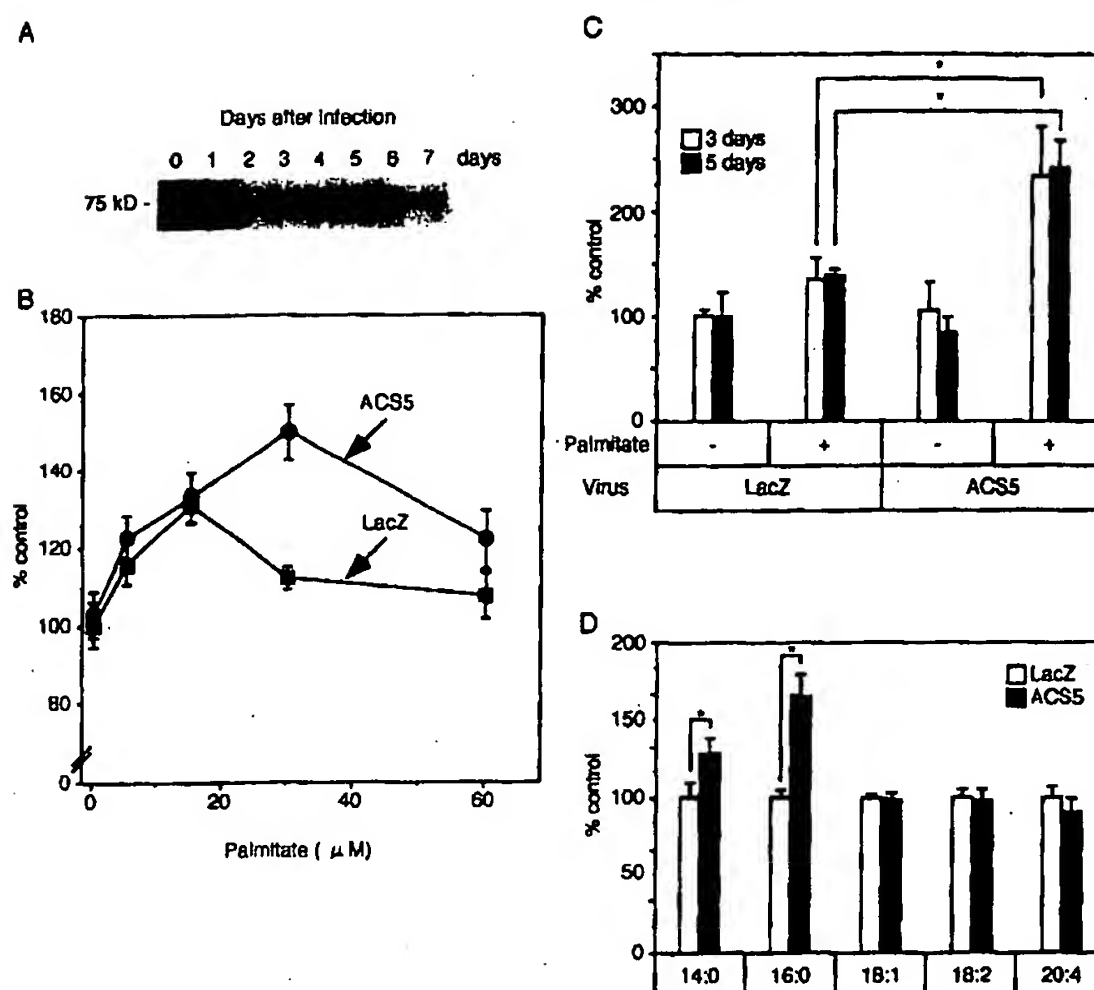


Figure 4 Fatty acid-induced glioma cell growth. (a) Immunoblot analysis of ACS5 in U87MG glioma cells after AdACSS infection. U87MG cells were infected with 5 moi of AdACSS, and 20 μ g of cell lysate was separated by SDS-PAGE, proteins were transferred to a nylon membrane, and ACS5 was detected with a polyclonal antibody against human ACS5. A representative time course change in the cellular levels of ACS5 in U87MG cells infected with AdACSS is shown. (b) Effects of increasing concentrations of palmitate on the growth of U87MG glioma cells infected with AdACSS. U87MG glioma cells infected with AdACSS or AdlacZ were cultured in DMEM supplemented with 10% FCS for 24 h, and then fed with DMEM supplemented with 2% FCS and 1% fatty acid free BSA for 24 h. Forty-eight hours after virus infection, cells were then cultured in DMEM containing 2% FCS, 1% fatty acid free BSA and with or without the indicated concentration of palmitate for 3 days. Data are presented as percentage of MTS value of mock-infected cells. Means \pm s.d. of quadruplicate determinations. (c) Fatty acid-induced glioma cell growth. U87MG glioma cells were infected with AdACSS or AdlacZ viruses and cultured as described above. Forty-eight hours after virus infection, cells were fed DMEM containing 2% FCS and 1% fatty acid free BSA with or without 30 μ M palmitate, and cultured for 3–5 days. Means \pm s.d. of quadruplicate determinations. *Statistical difference at $P < 0.05$. (d) Specificity of fatty acid-mediated growth stimulation of U87MG glioma cells infected with AdACSS or AdlacZ. Each fatty acid was added at 30 μ M together with 1% fatty acid free BSA in the presence of 2% FCS. After 96 h, cell numbers were obtained from quadruplicate wells. Fatty acids: 14:0, myristate; 16:0, palmitate; 18:1, oleate; 18:2, linoleate; 20:4, arachidonate. *Statistical difference at $P < 0.05$.

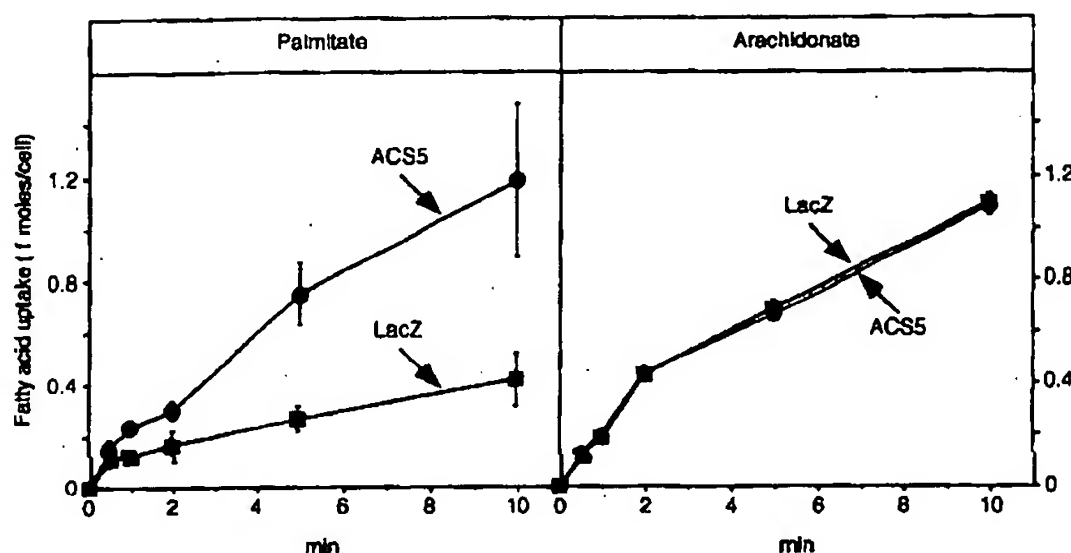


Figure 5 Fatty acid uptake by U87MG glioma cells infected with AdACSS or AdlacZ viruses. Forty-eight hours after virus infection, AdACSS and AdlacZ infected cells were assayed for uptake of [14 C]palmitate (left panel) and [14 C]arachidonate (right panel) as described in Materials and methods. Bars represent s.d. of quadruplicate determinations per time point.

Materials and methods

Molecular characterization of the human ACSS gene, cDNA and transcripts

Standard molecular biology techniques were used (Sambrook *et al.*, 1989). DNA sequencing was performed by the dideoxy chain-termination method on an Applied Biosystems model 373A DNA sequencer. For Northern blotting, total RNA prepared by the guanidinium thiocyanate/CsCl method was fractionated in a 1.5% agarose gel, transferred to a Zeta Probe nylon membrane (Bio-Rad, Hercules, CA, USA), and hybridized with 32 P-labeled probes. Quantitative analysis was performed with an image analyzer (BAS2000, Fuji Film, Tokyo, Japan) and expressed as the intensity of phosphostimulated luminescence. A human ACSS cDNA (designated phACSS) was obtained from a human liver cDNA library using the entire region of human rat ACSS cDNA (Oikawa *et al.*, 1998) as a probe. Bacterial artificial chromosome (BAC) and yeast artificial chromosome (YAC) clones containing the human ACSS genes were obtained by PCR-based screening of a BAC library (Genome Systems, St. Louis, MO, USA) and human genomic Mega YAC libraries A, B and C from the Centre d'Etude du Polymorphisme Humain (CEPH) (Cohen *et al.*, 1993), respectively. A set of human ACSS specific primers [5'-CTTCGGACCCAAATTGACAG-3' (nt. 2007-2027 of the (+) strand) and 5'-AAAGAAGAAGG-CACAGAGGGT-3' (nt 2392-2412 of the (-) strand)] were used for PCR-based screening under the conditions recommended for Ex TaqTM (Takara Shuzo Corp., Kyoto, Japan). Intron sizes were determined by Southern blotting, restriction mapping and PCR of the genomic clones. DNA fragments carrying exons were identified by restriction mapping and Southern blotting. After subcloning into pBluescript vectors, the sequences of exons, exon/intron boundaries and the 5'-flanking region were determined.

Human gliomas

Human glioma samples were obtained from 31 patients (21 men and 10 women) of ages 14–76 years at the time of surgical removal at the Department of Neurosurgery (Tohoku University School of Medicine). After obtaining written informed consent, DNA and RNA analyses were carried out, and these analyses were approved by the Institutional Review of Tohoku University School of Medicine. Total brain RNAs (four different lots) were obtained from Clontech laboratories, Inc. (Palo Alto, CA, USA) and used as normal controls.

Antibodies, immunohistochemistry and immunoblotting

A 15-residue peptide corresponding to amino acid residues 72 to 86 was synthesized by Nippon Gene Research Laboratories (Sendai, Japan). The amino acid composition and sequence were confirmed by the supplier. The peptide was coupled to keyhole limpet hemocyanin as described (Iijima *et al.*, 1996), and injected into rabbits according to the standard protocols (Harlow and Lane, 1988).

Immunohistochemical analysis of surgical specimens of grade IV malignant gliomas was performed on routinely processed, formalin-fixed, paraffin-embedded sections using a streptavidin-biotin complex method. The sections were autoclaved for 10 min before overnight incubation with a

human ACSS antibody (diluted 1:4000). The sections were washed and incubated with biotinylated secondary antibody (Histofine SAB-PO (M) kit, Nichiei, Tokyo, Japan). Detection was performed using 3',3-diaminobenzidine tetrahydrochloride (DAB). Sections were counterstained with hematoxylin.

For immunoblotting, protein samples were separated on 8% SDS-polyacrylamide gels and transferred to polyvinylidene difluoride membrane (Bio-Rad). The membrane was blocked by incubation for 4 h with 3% gelatin in phosphate buffered saline. The immunoblots were probed with human ACSS antibody (diluted 1:2000) and bound antibody was detected by horseradish peroxidase-conjugated anti-rabbit immunoglobulin G using an Enhance Chemiluminescence (ECL) Western Blotting Detection Kit (Amersham Pharmacia Biotech, Inc.).

Generation of a recombinant adenovirus containing human ACSS cDNA

An adenovirus (designated AdACSS) containing the entire region of human ACSS cDNA was generated by multiple ligations of restriction fragments using an adenovirus expression vector kit (Takara Shuzo). A recombinant adenovirus AdlacZ which contains modified chicken β -actin promoter with cytomegalovirus-immediate early promoter (Miyake *et al.*, 1996) and the β -galactosidase gene was used as a control. AdACSS and AdlacZ viruses were propagated in 293 cells, purified by CsCl ultracentrifugation, and stored in PBS containing 10% (w/v) glycerol at -80°C, according to the manufacturer's instructions.

Cell culture, virus infection, cell proliferation assay and fatty acid uptake

All lines of Glioma cells were maintained in DMEM supplemented with 10% FCS. For cell proliferation and fatty acid uptake assays U87MG cells were plated in microtiter plates. On day 0, cells were plated at 1×10^3 well and grown in DMEM supplemented with 10% FCS for 18 h and then infected with 5 moi of adenoviruses and further incubated for 24 h. On day 2, the medium was replaced by DMEM supplemented with 2% FCS and 1% BSA (fatty acid free). On day 3, cells were exposed to fatty acids in DMEM supplemented with 2% FCS and 1% BSA and cultured for 3–5 days for the cell proliferation assay. An MTS cell proliferation assay was performed using the CellTiter 96 Aqueous Non-Radioactive Cell Proliferation Assay (Promega Corp., Madison, WI, USA). For the fatty acid uptake assay, U87MG cells were cultured in DMEM supplemented with 10% FCS for 48 h after virus infection and washed with Dulbecco's complete (containing calcium and magnesium) phosphate buffered saline (PBS) and incubated with PBS containing 20 μ M BSA (fatty acid free) and 0.25 μ M [14 C]palmitate or 1 μ M [14 C]arachidonate. After incubation at 37°C for 1–10 min, cells were washed extensively at 4°C with PBS containing 0.1% BSA, solubilized with 1% SDS and counted for [14 C] uptake.

Acknowledgments

We thank Dr Ian Gleadall for critical reading of the manuscript. This work was supported by the Japan Society for the Promotion of Science Grant RFTF97L00803.

References

- Bergerheim US, Kunimi K, Collins VP and Ekman P. (1991). *Genes Chromo. Cancer*, **3**, 215–220.
- Bronfman M, Orellana A, Morales MN, Bieri F, Waechter F, Staubli W and Bentley P. (1989). *Biochem. Biophys. Res. Commun.*, **159**, 1026–1031.
- Coe NR, Smith AJ, Frohnert BI, Watkins PA and Bernlohr DA. (1999). *J. Biol. Chem.*, **274**, 36300–36304.
- Cohen D, Chumakov I and Weissenbach J. (1993). *Nature*, **366**, 698–701.

Fujino (1996)
Fujino 111;
Glick B
Grand I
Harlow
Mami
Henry T
Herbs (199-
Hertz K
Natu.
Iijima I
Yam Kang N
Nagu Natl.
Kurth VP
92. 1
Kuhajd
Dick
Sci. l
Miyake
Taka
Arad

Fujino T, Kang MJ, Suzuki H, Iijima H and Yamamoto T. (1996). *J. Biol. Chem.*, **271**, 16748–16752.

Fujino T and Yamamoto T. (1992). *J. Biochem. (Tokyo)*, **111**, 197–203.

Glick BS and Rothman JE. (1987). *Nature*, **326**, 309–312.

Grand RJ. (1989). *Biochem. J.*, **258**, 625–638.

Harlow E and Lane D. (1988). *Antibodies: A Laboratory Manual*. Cold Spring Harbor Laboratory: New York.

Henry MF and Cronan JJ. (1992). *Cell*, **70**, 671–679.

Herbst RA, Weiss J, Ehnis A, Cavenee WK and Arden KC. (1994). *Cancer Res.*, **54**, 3111–3114.

Hertz R, Magenheim J, Berman I and Bar-Tana J. (1998). *Nature*, **392**, 512–516.

Iijima H, Fujino T, Minekura H, Suzuki H, Kang MJ and Yamamoto T. (1996). *Eur. J. Biochem.*, **242**, 186–190.

Kang MJ, Fujino T, Sasano H, Minekura H, Yabuki N, Nagura H, Iijima H and Yamamoto TT. (1997). *Proc. Natl. Acad. Sci. USA*, **94**, 2880–2884.

Kabom AE, James CD, Boethius J, Cavenee WK, Collins VP, Nordenskjold M and Larsson C. (1993). *Hum. Genet.*, **92**, 169–174.

Kuhajda FP, Jenner K, Wood FD, Hennigar RA, Jacobs LB, Dick JD and Pasternack GR. (1994). *Proc. Natl. Acad. Sci. USA*, **91**, 6379–6383.

Miyake S, Makimura M, Kanegae Y, Harada S, Sato Y, Takamori K, Tokuda C and Saito I. (1996). *Proc. Natl. Acad. Sci. USA*, **93**, 1320–1324.

Oikawa E, Iijima H, Suzuki T, Sasano H, Sato H, Kamataki A, Nagura H, Kang MJ, Fujino T, Suzuki H and Yamamoto TT. (1998). *J. Biochem. (Tokyo)*, **124**, 679–685.

Peiffer SL, Herzog TJ, Tribune DJ, Mutch DG, Gersell DJ and Goodfellow PJ. (1995). *Cancer Res.*, **55**, 1922–1926.

Pizer ES, Chrest FJ, DiGiuseppe JA and Han WF. (1998). *Cancer Res.*, **58**, 4611–4615.

Rasheed BK, Fuller GN, Friedman AH, Bigner DD and Bigner SH. (1992). *Genes Chromo. Cancer*, **5**, 75–82.

Rasheed BK, McLendon RE, Friedman HS, Friedman AH, Fuchs HE, Bigner DD and Bigner SH. (1995). *Oncogene*, **10**, 2243–2246.

Sambrook J, Fritsch EF and Maniatis T (eds). (1989). *Molecular Cloning: A Laboratory Manual*, 2nd edn. Cold Spring Harbor Laboratory, Cold Spring Harbor, N.Y.

Schaffer JE and Lodish HF. (1994). *Cell*, **79**, 427–436.

Suzuki H, Kawarabayasi Y, Kondo J, Abe T, Nishikawa K, Kimura S, Hashimoto T and Yamamoto T. (1990). *J. Biol. Chem.*, **265**, 8681–8685.

Tomoda H, Igarashi K, Cyong JC and Omura S. (1991). *J. Biol. Chem.*, **266**, 4214–4219.

Yagasaki F, Jinnai I, Yoshida S, Yokoyama Y, Matsuda A, Kusumoto S, Kobayashi H, Terasaki H, Ohyashiki K, Asou N, Murohashi I, Bessho M and Hirashima K. (1999). *Genes Chromo. Cancer*, **26**, 192–202.

ONCOGENE ONCOGENE ONCOGENE ONCOGENE

Volume 19 • Number 51 • 30 November 2000

A Novel Acyl-CoA Synthetase, ACS5, Expressed in Intestinal Epithelial Cells and Proliferating Preadipocytes¹

Eisaku Oikawa,^{*2} Hiroaki Iijima,^{*} Takashi Suzuki,[†] Hironobu Sasano,[†] Hiroyuki Sato,^{*} Akihisa Kamataki,^{*} Hiroshi Nagura,[†] Man-Jong Kang,^{*} Takahiro Fujino,^{*} Hiroyuki Suzuki,^{*} and Tokuo T. Yamamoto^{*3}

^{*}Tohoku University Gene Research Center and [†]Department of Pathology, School of Medicine, Tohoku University, Sendai 981-8555

Received for publication, May 29, 1998

We report here the identification, characterization, and expression of a novel rat acyl-CoA synthetase (ACS) designated as ACS5. ACS5 consists of 683 amino acids and is approximately 60% identical to the previously characterized ACS1 and ACS2. ACS5 was overproduced in *Escherichia coli* cells and then purified to near homogeneity. The purified enzyme utilized a wide range of saturated fatty acids similar to those utilized by ACS1 and ACS2, but differed in its preference for C16-C18 unsaturated fatty acids. Northern blot analysis revealed that ACS5 mRNA is present most abundantly in the small intestine, and to a much lesser extent in the lung, liver, adrenal gland, adipose tissue, and kidney. *In situ* hybridization of rat ileum revealed abundant accumulation of ACS5 transcripts in foveolar epithelial cells. The hepatic level of ACS5 mRNA was significantly increased by refeeding a fat-free high sucrose diet and reduced by fasting or refeeding a high cholesterol diet, whereas that in the small intestine was not significantly altered by various dietary conditions. In contrast to the absence of ACS1 mRNA in undifferentiated 3T3-L1 preadipocytes, ACS5 mRNA was present in proliferating 3T3-L1 preadipocytes and its level remained unaltered during differentiation, suggesting that ACS5 may provide the acyl-CoA utilized for the synthesis of cellular lipids in proliferating preadipocytes.

Key words: acyl-CoA synthetase, dietary regulation, intestinal epithelial cell, lipogenesis, proliferation.

The ligation of fatty acids with coenzyme A (CoA) to produce acyl-CoA is a key reaction in mammalian fatty acid metabolism. This reaction, catalyzed by acyl-CoA synthetase (ACS, EC 6.2.1.3), is a crucial step in mammalian fatty acid metabolism, since mammalian fatty acid synthase contains a specific thioesterase to produce a free fatty acid as the final reaction product (1, 2). Therefore both *de novo* synthesized and dietary derived fatty acids cannot be metabolized without ACS in mammals. Acyl-CoA, the product of ACS, is utilized in various metabolic pathways including membrane biogenesis, energy production and fat deposition. Consistent with the multiple utilization of acyl-CoA, there are several ACSs in mammals.

¹This work was supported in part by research grants from the Ministry of Education, Science, Sports and Culture, the Ministry of Health and Welfare of Japan, and the Japan Society for the Promotion of Science. The nucleotide sequence(s) reported in this paper has been deposited in the GenBank™/EMBL Data Bank under accession number(s) AB012933.

²Present address: Water Quality Center, Environmental Headquarters, Maezawa Industries Inc., Kawaguchi 332-8556

³To whom reprint requests should be addressed. Phone: +81-22-717-8874, Fax: +81-22-263-9295, E-mail, yama@biochem.tohoku.ac.jp

Abbreviations: ACS, acyl-CoA synthetase; SREBP, sterol regulatory element binding protein.

© 1998 by The Japanese Biochemical Society.

In previous studies, we characterized four rat ACSs, designated as ACS1-4 (3-7). Although the four enzymes exhibit a structural architecture common to ACSs from various organisms, they can be classified into two subfamilies based on their structures and fatty acid preferences: one consists of ACS1 (3) and ACS2 (4), and the other of ACS3 (5) and ACS4 (6). Rat ACS1 and ACS2 share approximately 65% of their amino acids (4), and exhibit broad fatty acid specificities (7), but their tissue distributions are completely different: ACS1 is abundant in the liver, heart, and adipose tissue (3), whereas ACS2 is predominant in the brain (4). Between rat ACS3 and ACS4, approximately 68% of the amino acids are identical but they show poor amino acid identity with ACS1 and ACS2 (6). ACS3 utilizes laurate, myristate, arachidonate, and eicosapentaenoate most preferentially (5), whereas ACS4 prefers a narrow range of fatty acids including arachidonate, and eicosapentaenoate (6). ACS3 mRNA is expressed highly in the brain, and to a much lesser extent in the lung, adrenal gland, kidney, small intestine, and adipose tissue, but is not detected in the heart or liver (5). In contrast, the mRNA for ACS4 is expressed in steroidogenic tissues including the adrenal gland, ovary, and testis (6).

Although these ACSs exhibit different tissue distribution, none of them is preferentially expressed in the small intestine, where dietary lipids are hydrolyzed to free fatty acids in the lumen and absorbed by intestinal epithelial

cells. The absorbed free fatty acids are then converted to acyl-CoA for the synthesis of triacylglycerol and cholesterol esters in these cells, which enter the circulation as chylomicrons.

In the course of cDNA cloning of these four ACSs, we have isolated a cDNA encoding a fifth ACS. We describe here the primary structure, fatty acid preference, tissue expression, and regulation of this newly identified ACS, designated as ACS5.

EXPERIMENTAL PROCEDURES

Molecular Characterization of Rat ACS5—Standard molecular biology techniques were performed as described by Sambrook *et al.* (8). A rat liver cDNA library was constructed in the λ ZapII vector (Stratagene), using poly(A) RNA from rat liver, and screened with a 1.9 kb EcoRI/EcoRV fragment of rat ACS1 cDNA (3) as a probe under reduced hybridization conditions. On the screening of 1×10^6 clones, we obtained four positive clones, and one representative clone containing the largest cDNA insert (pACS5) was further characterized. The nucleotide sequences of cDNA fragments were determined by the dideoxy chain termination method (9) using M13 primers, T3 and T7, or specific internal primers. Sequence reactions were carried out using *Taq* DNA polymerase with fluorescently labeled nucleotides and an Applied Biosystems model 373A DNA sequencer.

For Northern blotting, total RNA prepared with acid-guanidinium thiocyanate-phenol-chloroform (10) was denatured with 1 M glyoxal and 50% dimethyl sulfoxide, electrophoresed on a 1.5% agarose gel, and then transferred to a nylon membrane (Zeta-Probe membrane; Bio-Rad). For normalization as to RNA loading, a 467 bp fragment of rat cyclophilin cDNA (11) was generated by reverse transcription-polymerase chain reaction (12) with nucleotide primers, 5'-TCAACCCACCCTGTTCTCGACAT-3' and 5'-GGTGATCTTCTTGCTGGTCTTGCCA-3', and used as a probe.

Construction of an ACS5 Expression Plasmid—Overproduction of ACS5 in *Escherichia coli* cells was carried out using a bacterial expression vector, pTV118N. To connect the second codon of the rat ACS5 cDNA (pACS5) adjacent to the initiator ATG of pTV118N, pACS5 was amplified by polymerase chain reaction using primer 1 (5'-CTTTTTAT-TTTAACTTGTT-3') and primer 2 (5'-AATACGACTCA-CTATAG-3'). The 2.3 kb PCR product was then digested with *Bam*HI, and the resulting 1.8 kb fragment was inserted into the *Nco*I (blunted)/*Bam*HI site of pTV118N. This intermediate plasmid was then digested with *Fba*I and *Pst*I, and ligated with a 2.1 kb *Fba*I/*Pst*I fragment of pACS5. The resulting expression plasmid (designated as pTV-ACS5) contains a *lac* promoter, an SD sequence and the entire coding region of ACS5 cDNA, and was used to transform *E. coli* cells, XL1-Blue.

Induction of the ACS Enzyme in *E. coli*—*E. coli* cells transformed with the ACS5 expression plasmid were grown in 1 liter of Terrific broth (1.2% Bacto Tryptone, 2.4% yeast extract, 0.4% glycerol, 90 mM potassium phosphate, pH 7.8) (8) supplemented with ampicillin (100 μ g/ml) and tetracycline (25 μ g/ml) at 30°C, and then induced by adding isopropyl- β -D-thio-galactopyranoside (IPTG) as described (7). After 12 h induction, the cells

were harvested and resuspended in 100 ml of buffer A [50 mM potassium phosphate, pH 7.4, 1 mM EDTA, 1 mM dithiothreitol, and 10% (w/v) glycerol] containing 1 mM phenylmethylsulfonyl fluoride. The resuspended cells were lysed by sonication and then centrifuged at 10,000 $\times g$ for 20 min at 4°C. The supernatant was taken as the crude extract and stored at -80°C until use.

Assay for ACS Activity—ACS activity was measured by either the isotopic method (13) or the spectrophotometric method (13); the latter was used only for the purified enzyme. Protein concentrations were determined by the Lowry method (14) with bovine serum albumin as a standard.

Purification of ACS5—A typical purification is described. All steps were carried out at 4°C. During the purification, the enzymes were monitored as to ACS activity.

The crude extract of the *E. coli* strain carrying pTV-ACS5 was further centrifuged at 105,000 $\times g$ for 90 min and the resulting precipitate was suspended in 40 ml of buffer B [buffer A containing 1% (w/v) Triton X-100] with 10 strokes of a Dounce homogenizer. The suspension was gently stirred for 1 h and then centrifuged at 105,000 $\times g$ for 1 h. The resulting supernatant was applied to a DEAE-Sephadex (Pharmacia) column (2.5 \times 10 cm) equilibrated with buffer B. The column was washed with three column volumes of the same buffer, and then eluted with a linear concentration gradient formed from four column volumes of buffer C [buffer A containing 0.1% (w/v) Triton X-100] and the same volume of buffer C containing 0.5 M NaCl. The pooled active fractions were concentrated with polyethylene glycol (PEG6000) and then dialyzed against buffer C.

In Situ Hybridization—Ileum specimens were obtained from 3-month-old male rats ($n=3$). The specimens were immediately fixed with 4% paraformaldehyde containing 0.5% glutaraldehyde for 18 h at 4°C and then embedded in paraffin wax. *In situ* hybridization was performed by use of a manual capillary action system (MicroProbe staining system; Fisher Scientific, Pittsburgh, PA), with modification of the reported methods (15, 16). The sequence of the 30-base ACS5 oligonucleotide probe used for *in situ* hybridization analysis was as follows: 5'-AGGTAAGACT-GGCTGAGGTCTGTTGATCAG-3', corresponding to 90 to 120 of ACS5. A sense oligonucleotide probe was used as a negative control. The probes were synthesized with a 3' biotinylated tail (Brigati tail) (5'-probe-biotin-biotin-biotin-TAG-TAG-biotin-biotin-biotin-3') as previously reported (17). Tissue sections (3 μ m, applied to Probe On Plus slides; Fisher Scientific) were hybridized with the anti-sense or sense oligonucleotide at 45°C for 1 h, washed twice with 2 \times SSC at 45°C (3 min per wash), and then incubated with alkaline phosphatase-conjugated streptavidin. After washing twice in AP Chromogen buffer (Research Genetics, Huntsville, AL) at room temperature, the hybridization products were visualized using Fast Red salt. The slides were counterstained with hematoxylin and air dried for light microscopic examination.

Animal Treatment—Male Wistar strain rats (six/group, caged together) weighing 200-300 g were used in the experiments. Control rats were fed on the commercial stock diet. Fasted rats were deprived of food for 48 h. Refed rats were fasted for 48 h followed by free access to a high

fat diet (10% soybean oil and 90% stock diet), a high cholesterol diet (2% cholesterol, 0.5% cholic acid, 10% soybean oil, and 87.5% stock diet) or a fat-free high sucrose diet (69% sucrose, 20% casein, 4% mineral mixture, 2% vitamin mixture, and 5% cellulose powder) for 72 h.

Cell Culture—3T3-L1 mouse preadipocytes (American Type Culture Collection) were maintained in Dulbecco's modified Eagle's medium (DMEM) supplemented with 10% fetal bovine serum, sodium ascorbate (0.2 mM), penicillin (50 U/ml), and streptomycin (50 µg/ml), with a change of the medium every 2-3 days. Differentiation of the preadipocytes was induced by shifting the cells, after confluence had been attained, to DMEM containing with 10% fetal bovine serum, 10 µg/ml insulin, 1 µM dexamethasone, and 0.5 mM methylisobutylxanthine. After 48 h, the medium was replaced with DMEM supplemented with insulin (5 µg/ml) and 10% fetal bovine serum.

RESULTS

A cDNA encoding a new type of ACS, designated as ACS5, was isolated from a rat liver cDNA library using rat ACS1 cDNA as a probe. Figure 1A shows the nucleotide and deduced amino acids sequences of the cDNA, which has an open reading frame of 2,049 bp corresponding of 683 amino acids (M_r 76,403). The putative initial methionine was preceded by an in-frame termination codon 81 nucleotides upstream.

ACS5, like other mammalian ACSs, consists of five regions: an N-terminal region, luciferase-like regions 1 and 2, a linker connecting the two luciferase-like regions, and a C-terminal region (Fig. 1B). Comparison of the amino acids in each of the five regions revealed that ACS5 belongs to the subfamily comprising ACS1 and ACS2: approximately 60% of the amino acids are identical to those in ACS1 and ACS2.

To overproduce ACS5 in *E. coli* cells, a bacterial expression plasmid containing a *lac* promoter and the entire coding region of the ACS5 cDNA was generated. The enzyme in the *E. coli* cells transformed with the expression plasmid was induced with isopropyl- β -D-thio-galactopyranoside and the resulting enzyme was purified to near homogeneity. The purification procedure involved solubilization of the enzyme with Triton X-100 and chromatography on DEAE-Sephadex (Table I). The overall purification was 39-fold, with a yield of 21.8%. The specific activity of the purified ACS5 was $5.1 \mu\text{mol}/\text{min}/\text{mg}$ when assayed with palmitate as a substrate. As shown on SDS-polyacrylamide gel electrophoresis (Fig. 2), the purified enzyme was nearly homogenous and had an apparent molecular mass of

TABLE I. Summary of the purification of recombinant ACS5. One liter of a culture of *E. coli* cells carrying pTV-ACS5 was used to prepare the crude extract. Enzyme activity was measured by the isotopic method using palmitate as a substrate.

Step	Total protein (mg)	Total activity ($\mu\text{mol}/\text{min}$)	Specific activity ($\mu\text{mol}/\text{min}/\text{mg}$)	Recovery (%)
Crude extract	2,842	369	0.13	100
140,000 $\times g$ pellet	184	221	1.2	59.9
Triton X-100 extract	145	174	1.2	47.2
DEAE-Sephadex	15.8	80.6	5.1	21.8

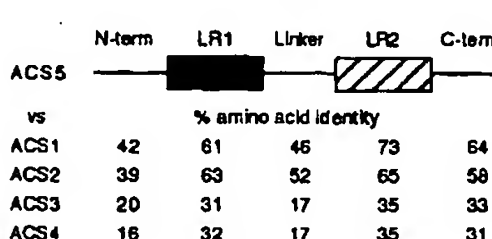


Fig. 1. Structure of rat ACS5 cDNA. (A) Nucleotide and deduced amino acid sequences of rat ACS5 cDNA. Nucleotide residues are numbered on the right and amino acids are numbered on the left. Nucleotide 1 is the A of the initiator AUG codon. Negative numbers refer to the 5'-untranslated region. Two in-frame translation termination codons, at -81 and 2050, are indicated by asterisks. A potential polyadenylation signal is underlined. (B) Comparison of the amino acids in rat ACS5 with those in the other four known rat ACSs. The five common regions in rat ACSs are shown in the upper portion: N-terminal region (N-term), luciferase-like region 1 (LR1), linker region (linker), luciferase-like region 2 (LR2), and C-terminal region (C-term). Figures indicate the percentage amino acid identities within each region of rat ACS1-4 compared with ACS5.

70 kDa, which is close to the molecular mass calculated from the deduced amino acid sequence of the cDNA.

Figure 3 compares the fatty acid preference of the purified recombinant ACS5 with that of ACS1 (7), as determined by the spectrophotometric method, using various fatty acids. Both the purified enzymes efficiently utilize saturated fatty acids with 12-18 carbon atoms and unsaturated fatty acids with 16-20 carbon atoms. Among these fatty acids, the best substrates are palmitic, palmitoleic, oleic, linoleic, and linolenic acids for ACS5, and palmitic acid for ACS1.

Northern blotting of RNA from various rat tissues revealed hybridization to a major transcript of 2.6 kb long, corresponding to pACS5 (Fig. 4). ACS5 transcripts are

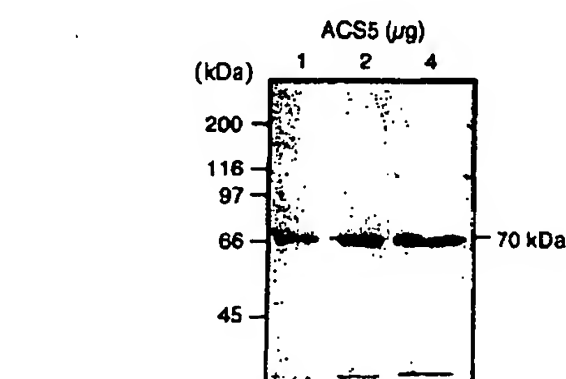


Fig. 2. SDS-polyacrylamide gel electrophoresis of the purified recombinant ACS5. 1, 2, and 4 μ g of the purified recombinant ACS5 were subjected to electrophoresis on an 8% SDS-polyacrylamide gel, and then staining with Coomassie Brilliant Blue R-250. Molecular size markers are indicated on the left.

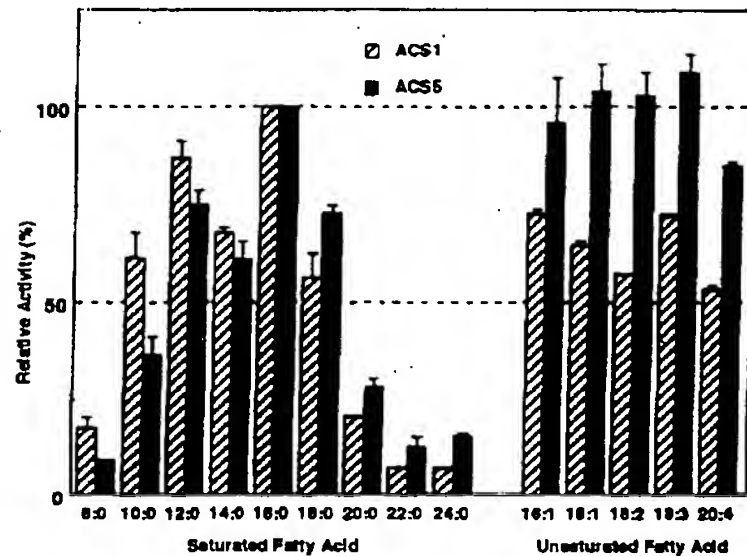


Fig. 3. Fatty acid specificity of the purified recombinant ACS5. Enzyme activity was determined by the spectrophotometric method with 1 μ g of the purified enzyme and the standard reaction mixture (13), except that various saturated and unsaturated fatty acids (final concentration, 0.1 mM) were used. Enzyme activity is expressed as a percentage of that obtained with palmitate as a substrate (5.1 μ mol/min/mg). The data represent the means \pm SD for triplicate determinations. Saturated fatty acids: 8:0, octanoic acid; 10:0, decanoic acid; 12:0, lauric acid; 14:0, myristic acid; 16:0, palmitic acid; 18:0, stearic acid; 20:0, arachidic acid; 22:0, docosanoic acid; 24:0, tetracosanoic acid. Unsaturated fatty acids: 16:1, palmitoleic acid; 18:1, oleic acid; 18:2, linoleic acid; 18:3, linolenic acid; 20:4, arachidonic acid.

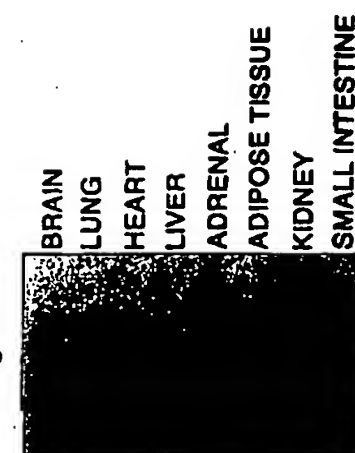


Fig. 4. Northern blot analysis of ACS5 mRNA in various rat tissues. Total RNA (15 μ g) prepared from the indicated rat tissues was subjected to electrophoresis on a 1.5% agarose gel, blotted onto a nylon membrane, and then hybridized with the 32 P-labeled 2.4 kb EcoRI/EcoRI fragment of pACS5. The filter was washed in 0.1 \times SSC containing 0.1% (w/v) SDS at 65°C for 30 min and then exposed to Kodak XAR-5 film with an intensifying screen at -80°C for 48 h. RNA loading was consistent among the lanes, as judged on ethidium bromide staining (data not shown). The autoradiograph shown is representative of four independent experiments which gave essentially identical results.

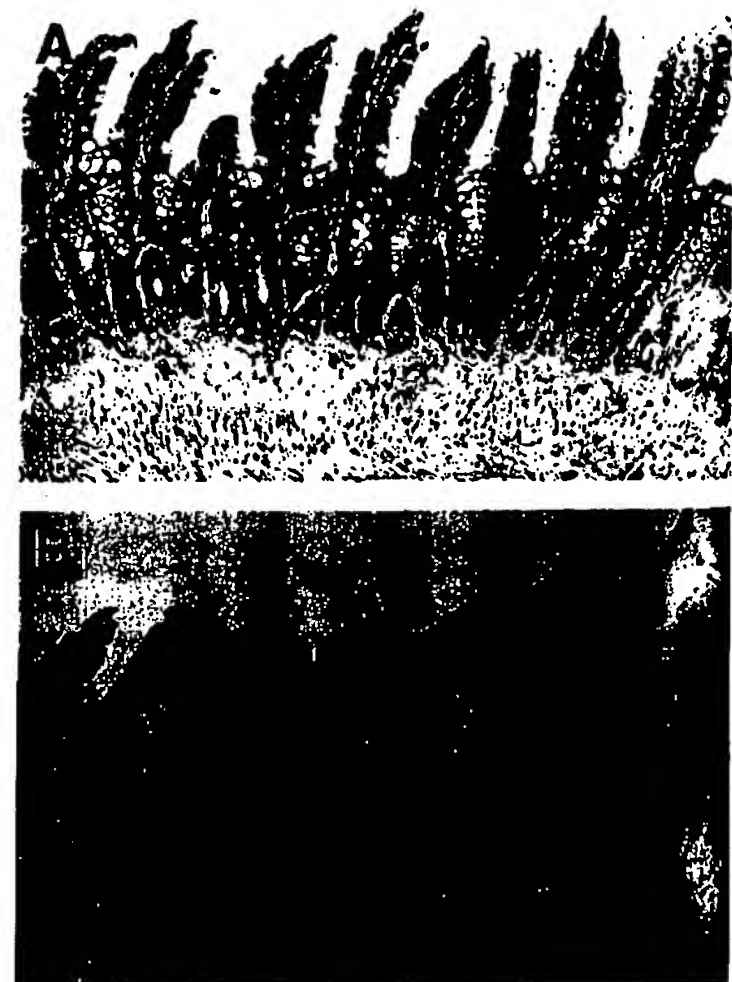


Fig. 5. *In situ* hybridization analysis of ACS5 transcripts in the rat ileum. Hybridization signals were visualized in red, as a result of the Fast Red salt, in the foveolar epithelial cells but not in the interstitial cells (A). The negative control with the sense oligonucleotide exhibited no accumulation of mRNA hybridization signals (B). Nuclei were made visible by counterstaining with hematoxylin. Magnification: 121 \times , A and B.

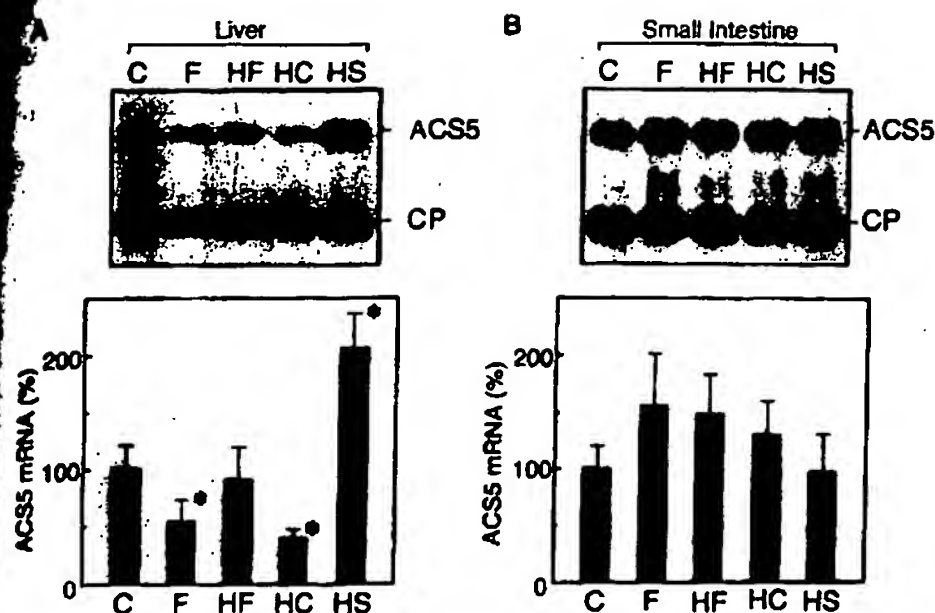


Fig. 6. Dietary effects on the hepatic and intestinal ACS5 mRNA levels. Total hepatic (A) and intestinal (B) RNA from rats ($n=6$) fed the control diet (C), fasted (F), and fed high fat (HF), high cholesterol (HC), and fat-free high sucrose (HS) diets were subjected to Northern blot analysis with rat ACS5 cDNA as described in the legend to Fig. 4, followed by autoradiography (exposed to XAR-5 film for 27 h). Northern blot analysis with a rat cyclophilin (CP) cDNA probe was carried out for normalization. The radioactivity in each band was quantified using a Bio-imaging Analyzer (BAS-2000, Fuji) with various exposure times and normalized as to the cyclophilin signal. The values in the lower panels are the means for six separate experiments \pm SD, relative to the mRNA level in control rats (set at 100). * $p < 0.01$ compared to the control.

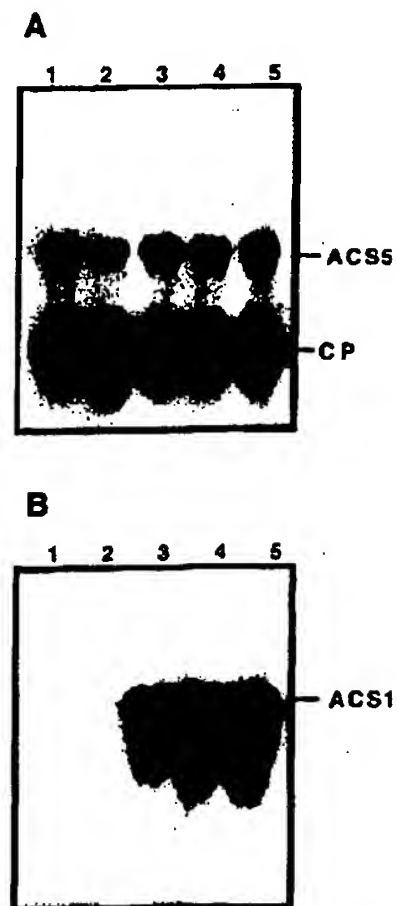


Fig. 7. Expression of ACS5 transcripts during the differentiation of 3T3-L1 cells. (A) 3-day postconfluent 3T3-L1 preadipocytes were harvested immediately prior to (lane 1), and 1 day (lane 2), 3 days (lane 3), 5 days (lane 4), and 7 days (lane 5) after differentiation. Total RNA (10 μ g) was analyzed by Northern blotting with the rat ACS5 (ACS5) and rat cyclophilin (CP) probes as described above, followed by exposure to Kodak XAR-5 film with an intensifying screen at -80°C for 18 h. (B) The same membrane as in (A) was hybridized with a 0.96-kb EcoRI/EcoRV fragment of rat ACS1 cDNA (pRACS15) and then exposed to Kodak XAR-5 film with an intensifying screen at -80°C for 12 h. The autoradiographs shown in (A) and (B) are each representative of four independent experiments that gave essentially identical results.

present most abundantly in the small intestine and to a much lesser extent in the lung, liver, adrenal, adipose tissue, and kidney in the normal adult rat (Fig. 4).

To locate cells expressing ACS5 mRNA, *in situ* hybridization was carried out using tissue sections prepared from adult rat ileum. Hybridization signals for ACS5 transcripts, appearing red as a result of the Fast Red reaction, were detected in the foveolar epithelial cells, but not in the interstitial cells (Fig. 5A). In negative controls for mRNA *in situ* hybridization using the sense oligonucleotide probe, no significant accumulation of ACS5 mRNA hybridization signals was detected (Fig. 5B).

A high level of hepatic ACS1 mRNA was induced by refeeding a high fat diet or a fat-free high sucrose diet after 48 h fasting (3). To determine the dietary effects on the level of ACS5 mRNA, Northern blotting was carried out using total RNA from the livers or small intestines of adult male rats fed various diets. Whereas the intestinal level of ACS5 mRNA was not altered significantly by various dietary conditions, that in the liver was significantly changed by fasting, or by refeeding a high cholesterol or fat-free high sucrose diet (Fig. 6). Fasting and refeeding a high cholesterol diet decreased the hepatic level of mRNA by 54 ± 17.5 and $39.2 \pm 7.8\%$, respectively. In contrast, refeeding a fat-free high sucrose diet increased the hepatic level of ACS5 mRNA approximately 2-fold.

We next determined the level of ACS5 mRNA during the differentiation of 3T3-L1 cells. As shown in Fig. 7, ACS5 transcripts were detected in undifferentiated proliferating adipocytes and their level was not altered during differentiation. In contrast, ACS1 transcripts were undetectable in undifferentiated proliferating adipocytes and markedly induced during differentiation.

DISCUSSION

In this study, we characterized a new ACS, designated as ACS5, that is abundantly expressed in intestinal epithelial cells. Although ACS5 resembles ACS1 and ACS2 in structure and substrate preference as to saturated fatty acids, the tissue distribution and regulation of its mRNA are completely different from those of ACS1 and ACS2. These

differences may reflect the biological roles of these three structurally similar ACSs, ACS1, ACS2, and ACS5.

In addition to the activation of fatty acids to form acyl-CoAs, ACS plays a role in the uptake of long-chain fatty acids, in cooperation with a fatty acid transporter (18). The abundant expression of ACS5 mRNA in intestinal epithelial cells suggests that it plays a part in the uptake of dietary derived fatty acids into these cells and their subsequent utilization. Consistent with this hypothesis, the purified recombinant ACS5 utilizes a wide range of saturated and unsaturated fatty acids.

Although the liver is not the major organ that expresses ACS5 mRNA, the regulation of the hepatic ACS5 mRNA level by various dietary conditions is noteworthy. Like that of ACS1 mRNA (3), the hepatic level of ACS5 mRNA was increased by refeeding a fat free high sucrose diet, but unlike that of ACS1 mRNA it was not induced by refeeding a high fat diet. It is also noteworthy that fasting and refeeding a high cholesterol diet significantly decreased the hepatic level of ACS5 mRNA. The induction of hepatic ACS5 mRNA by refeeding a fat-free high sucrose diet and reduction by fasting suggest that the plasma level of insulin may play a part in the regulation of the hepatic level of ACS5 mRNA: some of the lipogenic genes, including the acetyl-CoA carboxylase and fatty acid synthase genes, exhibit a similar pattern of dietary expression and are regulated by insulin (reviewed in Refs. 19 and 20). In addition, the induction of hepatic ACS5 mRNA by refeeding a fat-free high sucrose diet and the down regulation by refeeding a high cholesterol diet suggests transcriptional regulation of the mRNA by sterol regulatory element-binding proteins (SREBPs) (reviewed in Ref. 21). SREBPs are membrane-membrane bound transcription factors that mediate the synthesis of cholesterol and its uptake from low density lipoprotein in animal cells. In addition to the down regulation of genes involved in cholesterol metabolism, they also regulate the expression of genes encoding the enzymes for fatty acid metabolism (22, 23). Transgenic mice overproducing a truncated form of SREBP-1a exhibit massive liver enlargement due to increased synthesis of cholesterol and triglycerides (24). Therefore, it will be interesting to determine if hepatic transcription of the ACS5 gene is mediated by SREBPs and induced in transgenic mice overproducing a truncated form of SREBP-1a, since the metabolic fate of fatty acids is highly dependent on the activity of ACS enzymes.

The most interesting feature of ACS5 is the presence of its mRNA in proliferating preadipocytes. Although ACS1 mRNA is detected in a wide range of tissues, including liver and fat cells, it is not detected in either proliferating preadipocytes (25) or proliferating liver (26). Inhibition of ACS by specific inhibitors, triacins, profoundly reduces the synthesis of cellular phospholipids, thereby blocking the proliferation of mammalian cells (27). Therefore, ACS5 may provide the acyl-CoA required for the synthesis of cellular lipids during the proliferation of preadipocytes. Further studies are required to determine the exact role of ACS5 in lipid metabolism.

We wish to thank Dr. Ian Gleadall for critical reading of the manuscript, and Kyoko Ogamo-Karasawa and Nami Suzuki for their secretarial assistance.

REFERENCES

- Burton, D.N., Haavik, A.G., and Porter, J.W. (1968) Comparative studies on the rat and pigeon fatty acid synthetases. *Arch. Biochem. Biophys.* 126, 141-154
- Kumar, S. (1975) Functional deacylases of pigeon liver fatty acid synthetase complex. *J. Biol. Chem.* 250, 5150-5185
- Suzuki, H., Kawarabayasi, Y., Kondo, J., Abe, T., Nishikawa, K., Kimura, S., Hashimoto, T., and Yamamoto, T. (1990) Structure and regulation of rat long-chain acyl-CoA synthetase. *J. Biol. Chem.* 265, 8681-8685
- Fujino, T. and Yamamoto, T. (1992) Cloning and functional expression of a novel long-chain acyl-CoA synthetase expressed in brain. *J. Biochem.* 111, 197-203
- Fujino, T., Kang, M.-J., Suzuki, H., Iijima, H., and Yamamoto, T. (1996) Molecular characterization and expression of rat acyl-CoA synthetase 3. *J. Biol. Chem.* 271, 16748-16752
- Kang, M.J., Fujino, T., Sasano, H., Minekura, H., Yabuki, N., Nagura, H., Iijima, H., and Yamamoto, T.T. (1997) A novel arachidonate-preferring acyl-CoA synthetase is present in steroidogenic cells of the rat adrenal, ovary, and testis. *Proc. Natl. Acad. Sci. USA* 94, 2880-2884
- Iijima, H., Fujino, T., Minekura, H., Suzuki, H., Kang, M.J., and Yamamoto, T. (1996) Biochemical studies of two rat acyl-CoA synthetases, ACS1 and ACS2. *Eur. J. Biochem.* 242, 186-190
- Sambrook, J., Fritsch, E.F., and Maniatis, T. (1989) *Molecular Cloning: A Laboratory Manual*, 2nd ed., Cold Spring Harbor Laboratory, Cold Spring Harbor, NY
- Sanger, F., Nicklen, S., and Coulson, A.R. (1977) DNA sequencing with chain-terminating inhibitors. *Proc. Natl. Acad. Sci. USA* 74, 5463-5467
- Chomczynski, P. and Sacchi, N. (1987) Single-step method of RNA isolation by acid guanidinium thiocyanate-phenol-chloroform extraction. *Anal. Biochem.* 162, 156-159
- Danielson, P.E., Forss-Petter, S., Brow, M.A., Calavetta, L., Douglass, J., Milner, R.J., and Sutcliffe, J.G. (1988) p1B15: a cDNA clone of the rat mRNA encoding cyclophilin. *DNA* 7, 261-267
- Saiki, R.K., Gelfand, D.H., Stoffel, S., Scharf, S.J., Higuchi, R., Horn, G.T., Mullis, K.B., and Erlich, H.A. (1988) Primer-directed enzymatic amplification of DNA with a thermostable DNA polymerase. *Science* 239, 487-491
- Tanaka, T., Hosaka, K., and Numa, S. (1981) Long-chain acyl-CoA synthetase from rat liver. *Methods Enzymol.* 71, 334-341
- Lowry, O.H., Rosebrough, N.J., Farr, A.L., and Randall, R.J. (1951) Protein measurement with the Folin phenol reagent. *J. Biol. Chem.* 193, 265-275
- Iino, K., Sasano, H., Oki, Y., Andoh, N., Shin, R.W., Kitamoto, T., Totsune, K., Takahashi, K., Suzuki, H., Nagura, H., and Yoshimi, T. (1997) Urocortin expression in human pituitary gland and pituitary adenoma. *J. Clin. Endocrinol. Metab.* 82, 3842-3850
- Sasano, H., Uzuki, M., Sawai, T., Nagura, H., Matsunaga, G., Kashimoto, O., and Harada, N. (1997) Aromatase in human bone tissue. *J. Bone Miner. Res.* 12, 1416-1423
- Iezzoni, J.C., Kang, J.H., Montone, K.T., Reed, J.A., and Brigati, D.J. (1992) Colorimetric detection of herpes simplex virus by DNA in situ sandwich hybridization: a rapid, formamide-free, random oligomer-enhanced method. *Nucleic Acids Res.* 20, 1149-1150
- Schaffer, J.E. and Lodish, H.F. (1994) Expression cloning and characterization of a novel adipocyte long chain fatty acid transport protein. *Cell* 78, 427-436
- Iritani, N. (1992) Nutritional and hormonal regulation of lipogenic enzyme gene expression in rat liver. *Eur. J. Biochem.* 205, 433-442
- Girard, J., Perdereau, D., Foufelle, F., Prip-Buus, C., and Ferre, P. (1994) Regulation of lipogenic enzyme gene expression by nutrients and hormones. *FASEB J.* 8, 36-42
- Brown, M.S. and Goldstein, J.L. (1997) The SREBP pathway: regulation of cholesterol metabolism by proteolysis of a mem-

brane-bound transcription factor. *Cell* 89, 331-340

2. Bennett, M.K., Lopez, J.M., Sanchez, H.B., and Osborne, T.F. (1995) Sterol regulation of fatty acid synthase promoter. Coordinate feedback regulation of two major lipid pathways. *J. Biol. Chem.* 270, 25578-25583

3. Lopez, J.M.; Bennett, M.K., Sanchez, H.B., Rosenfeld, J.M., and Osborne, T.E. (1996) Sterol regulation of acetyl coenzyme A carboxylase: a mechanism for coordinate control of cellular lipid. *Proc. Natl. Acad. Sci. USA* 93, 1049-1053

24. Shimano, H., Horton, J.D., Hammer, R.E., Shimomura, I., Brown, M.S., and Goldstein, J.L. (1996) Overproduction of cholesterol and fatty acids causes massive liver enlargement in transgenic mice expressing truncated SREBP-1a. *J. Clin. Invest.* 98, 1575-1584

25. Amri, E.Z., Ailhaud, G., and Grimaldi, P. (1991) Regulation of adipose cell differentiation. II. Kinetics of induction of the aP2 gene by fatty acids and modulation by dexamethasone. *J. Lipid Res.* 32, 1457-1463

26. Schoonjans, K., Staels, B., Grimaldi, P., and Auwerx, J. (1993) Acyl-CoA synthetase mRNA expression is controlled by fibrin-acid derivatives, feeding and liver proliferation. *Eur. J. Biochem.* 216, 615-622

27. Tomoda, H., Igarashi, K., Cyong, J.C., and Omura, S. (1991) Evidence for an essential role of long chain acyl-CoA synthetase in animal cell proliferation. Inhibition of long chain acyl-CoA synthetase by triacins caused inhibition of Raji cell proliferation. *J. Biol. Chem.* 266, 4214-4219

第124巻第3号 1998年9月1日発行(毎月1回1日発行)
9月9日第三種郵便物認可



VOLUME 124, NO. 3
SEPTEMBER 1998

THE JOURNAL OF BIOCHEMISTRY

BIOCHEMISTRY

MOLECULAR BIOLOGY

CELL

BIOTECHNOLOGY

The JB is available on the Web at:
<http://JB.I.casj.or.jp>

Published Monthly by
THE JAPANESE BIOCHEMICAL SOCIETY
ISSN 124(3)473-686(1998)

Impaired Expression of Acyl-CoA-Synthetase 5 in Epithelial Tumors of the Small Intestine

NIKOLAUS GASSLER, MD, ARMIN SCHNEIDER, MD, JÜRGEN KOPITZ, PhD,
MARTINA SCHNÖLZER, PhD, NICHOLAS OBERMÜLLER, MD,
JÜRGEN KARTENBECK, PhD, HERWART F. OTTO, MD,
AND FRANK AUTSCHBACH, MD

Fatty acids are implicated in tumorigenesis, but data are limited concerning endogenous fatty acid metabolism of tumor cells in adenomas and adenocarcinomas of the small intestine. The recently cloned human acyl-CoA-synthetase 5 (ACS5) is predominantly found in the small intestine and represents a key enzyme in providing cytosolic acyl-CoA thioesters. Protein synthesis and mRNA expression of ACS5 were studied in human intestinal tissues using different methods, including a newly established monoclonal antibody. In the healthy small intestine, expression of ACS5 was restricted to the villus surface epithelium but was not detectable in enterocytes lining crypts. ACS5

In contrast to epithelial tumors of the large intestine, adenomas and adenocarcinomas of the small intestinal mucosa are rare, and this occurs despite the fact that approximately 90% of the mucosal surface of the gastrointestinal tract is concentrated in the small intestine.¹ The reasons for this discrepancy may lie in the rapid turnover of the small intestinal mucosa, the relative absence of bacteria, the alkaline pH, the decreased transit time, and the well-developed local immunoglobulin A (IgA)-mediated immune system. Moreover, the nutritional content is much more diluted in the small intestine than is the case in the large bowel.² Carcinomas of the small and large intestine share morphological characteristics, and they both may arise from adenomas of the intestinal mucosa. The progression to invasive cancer of the intestine is generally termed the *adenoma-carcinoma sequence* and is accompanied by a series of genetic, functional, and morphological changes.³ It has been suggested that the genetic pathway of carcinomas of the small intestine is different in detail from that found in colorectal cancer. Moreover, it has been hypothesized that the small bowel is more resistant to genetic events.³ With regard to this assumption, we focused our work on a specific enzyme, the

protein and mRNA were progressively diminished in epithelial cells of adenomas and adenocarcinomas of the small intestine. In conclusion, altered expression of ACS5 is probably related to the adenoma-carcinoma sequence of small intestinal epithelial tumors due to an impaired acyl-CoA thioester synthesis. HUM PATHOL 34:1048-1052. © 2003 Elsevier Inc. All rights reserved.

Key words: carcinoma, epithelial tumors, fatty acid metabolism, small intestine.

Abbreviations: ACS5, acyl-CoA-synthetase 5; mAb, monoclonal antibody.

intestinal acyl-CoA-synthetase 5 (ACS5), which is preferentially expressed in the small intestinal mucosa. The ACS5 molecule is a member of a protein family that plays a crucial role in fatty acid metabolism, mainly by the generation of multifunctional long-chain-fatty-acid-CoA esters.⁴ However, ACS5 might also be involved in the regulation of several biochemical pathways and genes by synthesis of long-chain-acyl-CoA thioesters.

Long chain acyl-CoA thioesters have been reported to affect a large number of intracellular functions and biosystems including ion pumps and channels, enzymes, lipid biosynthesis, and fatty acid degradation.⁵ Apart from these basal functions, long chain acyl-CoA esters have important functions in the regulation of intermediary metabolism and gene expression.⁶ In *Escherichia coli*, acyl-CoA esters have been characterized to be the regulatory ligands of FadR, a global transcription factor regulating the expression of genes involved in fatty acid biosynthesis or degradation, respectively.⁷ In the absence of acyl-CoA esters, FadR directly binds to specific DNA sequences. Binding of acyl-CoA leads to strong conformational changes throughout the FadR protein, resulting in a rearrangement of the DNA-binding domains, with subsequent loss of DNA binding.⁸ Evidence has accumulated indicating that acyl-CoA-binding proteins that affect gene transcription also exist in higher organisms.⁹

The aim of this study was to identify and to locate the expression and synthesis of the enzyme ACS5 in the small intestine of humans. We also wanted to rule out whether ACS5 expression differs between the healthy small intestinal mucosa and epithelial tumors (adenomas and adenocarcinomas) of the small intestine.

MATERIALS AND METHODS

Patients

A total of 20 small intestinal samples (10 men, 10 women; range, 30 to 87 years) were included in the study, comprising

From the Department of Pathology, Heidelberg and the Department of Pathochemistry, University of Heidelberg, Heidelberg; Axarion Bioscience AG, Heidelberg; and Protein Analysis Facility and Division of Cell Biology, Deutsches Krebsforschungszentrum, Heidelberg; and the Division of Nephrology, Medical Clinic IV, University of Frankfurt/Main, Frankfurt, Germany. Accepted for publication June 19, 2003.

Supported by grants from Tumorzentrum Heidelberg/Mannheim (I.I.2.) and Deutsche Forschungsgemeinschaft (SFB 405; B6).

Address correspondence and reprint requests to Dr Nikolaus Gassler, Department of Pathology, University of Heidelberg, INF 220/221, 69120 Heidelberg, Germany.

© 2003 Elsevier Inc. All rights reserved.
0046-8177/03/3410-0018\$30.00/0
doi:10.1053/S0046-8177(03)00491-3

15 adenocarcinomas (9 men, 6 women; mean age, 72 years; range, 54 to 87 years) and 5 well-differentiated adenomas (1 man, 4 women; mean age, 49 years; range, 30 to 74 years). For molecular procedures, reference small intestinal tissues were used from surgical resections for cancer of the ascending colon (1 man, 4 women; mean age, 61 years; range, 33 to 80 years). Mucosal tissue layers were mechanically dissected, immediately cooled in liquid nitrogen, and stored at -80°C until use. All diagnoses were established independently by two authors (F.A. and N.G.) by conventional histological criteria on hematoxylin and eosin-stained sections of paraffin-embedded tissues. The use of human tissues was approved by Heidelberg University.

Generation of the Monoclonal Antibody KD7 Against ACS5

Six booster immunizations of a Sprague Dawley rat (Janvier, Le Geneste-St. Isle, France) was performed over 80 days using a liquid preparation of unaffected purified human small intestinal epithelium including the mature ACS5 protein in the presence of complete Freund's adjuvant (Sigma, Deisenhofen, Germany). Splenic B cells were subsequently fused with P3X63Ag8 tumor cells from BALB/c mouse (CRL-1597; ATCC, Manassas, VA) to produce hybridomas. Undiluted supernatants of single clones were used for immunofluorescence screens on tissue sections of human small intestine. Hybridomas showing mucosal signals were subcloned twice and tested again. The monoclonal antibody (mAb) named KD7 was purified by antibody affinity chromatography using a HiTrap Protein G HP column according to the manufacturer's instructions (Amersham Pharmacia Biotech, Little Chalfont, England).

Fast Protein Liquid Chromatography

Homogenates of purified reference small intestinal mucosal tissues solubilized in Laemmli sample buffer were separated by 7.5% sodium dodecyl sulfate-polyacrylamide gel electrophoresis (SDS-PAGE). Eluted proteins were concentrated by chloroform-methanol (1/4, v/v) precipitation, extracted with 0.1% *tri*-fluoroacetic acid (TFA), and separated by ultracentrifugation (430,000 $\times g$, 4°C, 15 minutes). The supernatants were applied to a fast-protein liquid chromatography (FPLC) system that was equipped with a Resource RPC column (3 mL; Amersham Pharmacia Biotech). A gradient of the following solvent mixtures was used: solvent A, 0.1% TFA in water; solvent B, 0.1% TFA in acetonitrile. The gradient elution program at 20°C consisted of the following: 5 minutes of solvent A; a linear gradient from solvent A to A/B (50/50) over 15 minutes; 2 minutes with A-B (50/50); a linear gradient from A-B (50/50) to A-B (20/80) over 10 minutes; a linear gradient from A-B (20/80) to solvent B (1 minute); and 2 minutes with solvent B. FPLC-purified fractions were collected in 0.5-mL samples and further evaluated by Western blot and matrix-assisted laser desorption and ionization (MALDI) mass spectrometry (see MALDI Mass Spectrometry).

MALDI Mass Spectrometry

FPLC-purified proteins were separated by SDS-PAGE, and the protein band (~68 kDa) recognized by the mAb KD7 was excised from the 7.5% PAA gel. MALDI mass spectra were recorded in the positive ion reflector mode on a Reflex II time-of-flight instrument (Bruker-Daltonik GmbH, Bremen, Germany). Sample preparation for PSD analysis was achieved

by cocrystallization of alpha-cyano-4-hydroxycinnamic acid saturated in 50% acetonitrile-water with ZipTip C18 (Millipore, Bedford, MA). PSD spectra (positive ion reflector mode; ion gate width of 40 Da around the ion of interest) were generated, acquired in 14 segments by decreasing the reflector voltage (100 to 200 individual laser shots per segment). Searches were performed against the National Center for Biotechnology Information (NCBI) database.

SDS-PAGE and Western Blot Analysis

Mucosal samples of the small intestine were homogenized in TRI reagent (Sigma, Deisenhofen, Germany) using the Ultra Turrax equipment (IKA Labortechnik, Staufen, Germany) and extracted according to the manufacturer's recommendations. The BioRad assay reagent were used for protein measurements according to the manufacturer's suggested protocol (BioRad, München, Germany). The final preparation in Laemmli buffer was stored at -20°C until use. Proteins were separated by 1-dimensional SDS-PAGE (7.5%) and transferred to a PVDF Immobilon-P membrane (Millipore) by semi dry blotting. In addition to mAb KD7, the following antibodies were used: mouse anti-rat IgG1, mouse anti-rat IgG2a, and mouse anti-rat IgG2b (each, 1:250; all antibodies from Serotec, Oxford, UK); horseradish peroxidase-conjugated anti-mouse or anti-rat antibodies, respectively (1:10,000; Santa Cruz, Santa Cruz, CA). The enhanced chemiluminescence substrate (Amersham Pharmacia Biotech) was applied according to the manufacturer's recommendations. Negative controls included blots in which the primary antibody was omitted.

Reverse Transcription

Reverse transcription was performed using the SuperScript II amplification system for first-strand cDNA synthesis according to the manufacturer's suggestions (Invitrogen/Life Technologies, Karlsruhe, Germany). Five micrograms of DNase-digested total RNA isolated from small intestinal mucosa was used for oligo (dT)-primed first-strand cDNA synthesis. Reverse transcription was terminated at 70°C for 15 minutes, followed by an RNase H digestion (20 minutes at 37°C). In control experiments, transcription of a commercially provided control RNA (50 ng) was performed in which the enzyme reverse transcriptase was substituted by distilled water.

Cloning and Expression of Human ACS5 and ACS2 in E. Coli M15

Human ACS5 (accession no. NM_016284) and ACS2 (accession no. NM_021122) were amplified using a set of designed primers: ACS5 upper primer, 5'-Pho-ATG CTT TTT ATC TTT AAC TTT TTG TTT TCC CCA C-3'; ACS5 lower primer, 5'-ACG AGC TCG GAT CCT AAT CCT GGA TGT GCT CAT ACA G-3'; ACS2 upper primer, 5'-Pho-ATG CAA GCC CAT GAG CTG TTC C-3'; ACS2 lower primer, 5'-ACG AGC TCG GAT CCT AAA CCT TGA TAG TGG AAT AGA GGT C-3' and Vent DNA Polymerase (NEB, Frankfurt/Main, Germany) according to the manufacturer's suggestion. The PCR products were digested with *Bam*HI and then ligated into a dephosphorylated *Stu*I-*Bam*HI digest of pQE-30Xa (Qiagen, Hilden, Germany) and afterward transformed into *E. coli* M15 (Qiagen). Expression of ACS5 was induced by application of IPTG (Sigma).

DNA Sequencing

Sequencing of full-length cDNA clones (6xHis-tagged construct) was performed using 300 ng of plasmid DNA and 10 pmol of appropriate primers (pQE forward and reverse vector primers and internal sequencing primers). All reactions were run on an ABI 3700 capillary sequencer according to the manufacturer's recommendations (ABI, Weiterstadt, Germany).

mRNA In Situ Hybridization

A 970-bp PCR product covering exon 21 and an untranslated region of human ACS5 were amplified using the primers 5'-CAA CAT TGA AAC CAA AGC GA-3' and 5'-AAT AAG CCT GTT GTC TGG GC-3'. The amplicon was cloned into the PCR-bluntII-topo vector using Topo TA cloning (Invitrogen/Life Technologies), and the orientation of inserts was determined by end sequencing. Plasmids were restricted with *Bam*HI and then transcribed with T7 RNA polymerase (Roche, Mannheim, Germany). Deparaffinized tissue sections were treated with proteinase K (Roche; 10 µg/mL; 30 min at 37°C) and acetylated. The transcripts were shortened by alkaline hydrolysis. Hybridization with a probe concentration of 4 ng/µL hybridization mixture was carried out overnight at a temperature of 46°C. Controls included tissue sections in which the antisense probe or the anti-digoxigenin antibody were replaced by the sense probe or PBS, respectively.

Immunohistochemistry

For immunohistochemistry on paraffin-embedded tissues, the ABC detection kit with DAB as the chromogen was used in accordance to the manufacturer's suggested protocols (DAKO, Glostrup, Denmark). Negative controls included sections in which the appropriate reference serum was used.

RESULTS

ACS5 Is Recognized by the mAb KD7

The protein recognized by the mAb KD7 was characterized as follows. At first, FPLC-purified small intestinal mucosal proteins were analyzed by Western blot procedure, by which a single band with a molecular mass about 68 kDa was detected (Fig 1A, column I). This single protein band was isolated and further identified as human ACS5 by the MALDI technique (NCBI database no. AB033920). Second, the mAb KD7 recognized the recombinant human ACS5 protein as a single band in Western blot analysis (Fig 1A, column II), but not the recombinant human ACS2 protein. Among the ACSs, ACS2 with about 60% homology at the amino acid level shares the highest similarity with ACS5. The mAb KD7 was further characterized as IgG2b by isotype-specific mapping (Fig 1A, column III).

Expression of ACS5 in Reference Human Small Intestine

In the reference small intestine, ACS5 protein and mRNA were exclusively located to the villus epithelium, whereas they were absent from crypts (Fig 1B and C). At the villus, a continuous cytoplasmic staining of the epithelium was observed, including enterocytes, goblet

cells, and endocrine cells. In the large intestine, only cells of the apical surface epithelium displayed a weak immunostaining of ACS5. As with the small intestine, immunosignaling was not found in the crypt epithelium (data not shown).

Expression and Synthesis of ACS5 Is Impaired in Small Intestinal Adenomas

The immunohistochemical studies revealed a loss of ACS5 protein in adenomas of the small intestine ($n = 5$). Reference enterocytes in the vicinity of adenomas displayed a strong expression of ACS5. The immunohistochemical data were corroborated by the mRNA in situ hybridization experiments (Fig 1D through F).

Expression and Synthesis of ACS5 Is Impaired in Small Intestinal Adenocarcinomas

In all adenocarcinomas analyzed ($n = 15$), ACS5 protein and mRNA were not detectable in the majority of tumor cells. Occasionally, clusters of tumor cells displayed a weak immunostaining against ACS5 and very small amounts of ACS5 mRNA were found (Fig 1G through J). These cells were located within the adenocarcinomas and showed morphological criteria of malignancy including cellular and nuclear pleomorphy. Interestingly, ACS5 was never seen in mitotic tumor cells. The strong ACS5 expression found in morphological reference enterocytes at the periphery of adenocarcinomas served as an internal control.

DISCUSSION

The systematic analyses of the hybridoma library led to the identification of a highly abundant protein of the small intestinal mucosa, the recently cloned ACS5.⁴ Here we show that ACS5 shows an expression gradient with weak expression levels in the crypts of Lieberkühn but strong expression in the villus lining epithelium, which is in good agreement with data obtained for the rat homologue of ACS5.¹⁰ This concordance, as well as the inability of mAb KD7 to detect the ACS isoform ACS2, strongly argues for the specificity of the monoclonal antibody. Experimental evidence from Western blot analyses and real-time PCR (LightCycler, Roche, Mannheim, Germany) is given that ACS5 protein and mRNA are preferentially found in the small, but not in the large intestine (data not shown).

ACS5s catalyze the synthesis of acyl-CoA, which is the initial step required for oxidation, elongation, and desaturation of fatty acids; for the synthesis of complex lipids and acylated proteins; as well as for a variety of signals that regulate cellular metabolism and gene expression. It has been recognized that fatty acids have a significant effect on mRNA abundance of genes encoding proteins involved in fatty acid metabolism.^{6,8,11} Fatty acids suppress fatty acid synthetic enzymes, including acetyl-CoA carboxylase and ATP-citrate lyase, whereas they increase expression of genes involved in

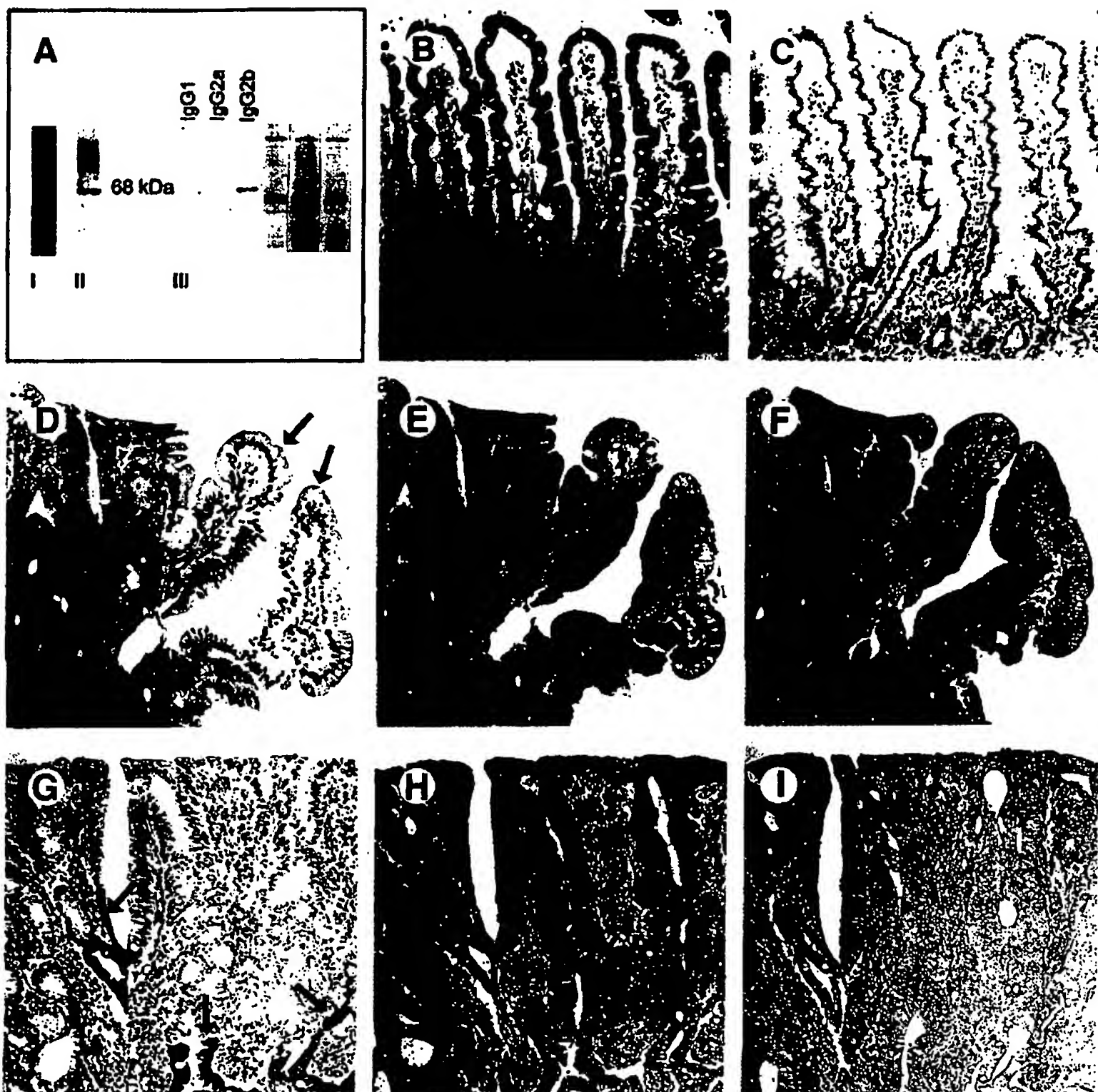


FIGURE 1. Characterization of the monoclonal antibody against acyl-CoA-synthetase 5 (ACSS5; A to C) as well as serial sections of paraffin-embedded tissues of a tubular adenoma (D through F) and an adenocarcinoma (G through I) of the small intestine after DAB immunostaining (D and G) or mRNA *in situ* hybridization (E, F, H, and I) of acyl-CoA-synthetase 5, respectively. (A) Column I, FPLC-purified ACSS5 as well as (column II) the recombinant human ACSS5 are recognized by the monoclonal antibody KD7; (column III) The mAb KD7 is characterized as IgG2b by isotype-specific mapping. (B) In reference small intestine, strong DAB immunostaining of ACSS5 is found in enterocytes at villi, but not in crypts. (C) Similarly processed section as that shown in (B) in which the monoclonal antibody KD7 had been totally omitted and replaced by the appropriate Immunoglobulin fraction (negative control). (D) Tubular adenoma of the small intestine. The immunostaining of ACSS5 is highly diminished in tumor cells, whereas ACSS5 expression is preserved in reference enterocytes (arrows). (E) Serial section of (D) after mRNA *in situ* hybridization against ACSS5 with an identical distribution of the ACSS5 mRNA as shown for the ACSS5 protein. (F) Serial tissue section from (E) and (D) after mRNA *in situ* hybridization using digoxigenin-labeled sense riboprobes to ACSS5 (control). (G) Adenocarcinoma of the small intestine after DAB immunostaining against the ACSS5. In the majority of tumor cells, the immunostaining of ACSS5 protein is very weak. ACSS5 expression is preserved in reference enterocytes (arrows). (H) Serial section of (G) after mRNA *in situ* hybridization against ACSS5. The distribution of the ACSS5 mRNA is identical to that shown for the ACSS5 protein. (I) Serial tissue section from (G) and (H) after mRNA *in situ* hybridization using sense riboprobes to ACSS5 (control). Original magnification: B and C, $\sim \times 20$; D through I, $\sim \times 40$.

peroxisomal biogenesis and β -oxidation. However, it has been suggested that the regulatory effect of acyl-CoA esters is not restricted to bacteria and yeast.^{6,12,13}

The concentration of acyl-CoA esters in the cell cytosol is controlled by several factors including long-chain fatty acid synthesis and consumption, the concentration of acyl-CoA and fatty acid-binding protein, as well as acyl-CoA hydrolase and sterol carrier protein 2 activity.¹¹ Acyl-CoA thioester can also be expected to bind to further proteins in the cytoplasm, including the high-affinity binding site on acyl-CoA synthetases and other acyl-CoA-utilizing enzymes. Taking all of the above considerations into account, the intracellular free acyl-CoA concentration will be in the range of 0.1 to 200 nmol/L.^{5,11} When looking at the high binding capacity for intracellular long-chain fatty acids, large fluctuations of these molecules are not to be expected under reference physiological conditions. In contrast, impaired fatty acid metabolism has been recorded in tumor cells, and experimental data point to a relationship between abnormal fatty acid synthesis and an aggressive tumor phenotype.¹⁴

Our data give clear evidence that expression and synthesis of ACS5 is reduced in adenomas and adenocarcinomas of the small intestine when compared with the reference small intestinal mucosa. Therefore we speculate that the synthesis of acyl-CoA and consequently the intracytoplasmic level of acyl-CoA might be impaired in tumor cells, which is in accordance with data previously published.¹⁴ The reduced expression of ACS5 mRNA and protein observed in tumor cells of the small intestine should be discussed as one mechanism for impaired acyl-CoA synthesis that could influence gene expression related to tumorigenesis. It has been suggested that tumor cells use lipid mediators that may act as autocrine or paracrine factors, ultimately affecting the tumor behavior.¹⁴ Thus, the possibility should be taken into consideration that the reduction of ACS5 expression in adenomas may precede progress in carcinogenesis. Within this scenario, it could also represent one of the possible initial steps in tumorigenesis, for example, by creating a local environment that temporarily lacks acyl-CoA thioesters. To test this hypothesis and to rule out the possibility that modulation of ACS5 may be an incidental epiphenomenon, further functional studies are required.

Our study does not rule out the possibility that other acyl-CoA-synthetase isoforms than isoform 5 are expressed and synthesized by the neoplastic epithelial cells of adenomas and adenocarcinomas of the small intestine. This possibility does appear to be of interest, because certain tumors have an apparently obligatory requirement for endogenous fatty acid biosynthesis. Moreover, the expression of ACS5 could be suppressed by high cytosolic levels of acyl-CoA esters of other origin. In our study, ACS5 protein and mRNA was exclusively investigated by *in situ* experiments on tissue sections of paraffin-embedded epithelial tumors of the small intestine. True quantification of ACS5 and other acyl-CoA-synthetase isoforms is not given by these methods, and *in situ* data have to be substantiated by other

techniques, like Western blot analysis, enzyme-linked immunosorbent assay, or quantitative reverse-transcription-polymerase chain reaction. Unfortunately, the application of all of these methods was limited, because only paraffin-embedded, formalin-fixed tissues were available for our investigations.

In conclusion, our data relate the enzyme ACS5 to the adenoma-carcinoma sequence of small intestinal epithelial tumors. The decrease of ACS5 protein and mRNA in tumor cells are probably related to an impaired acyl-CoA thioester synthesis that could be of relevance concerning tumorigenesis in the small intestine. To test this hypothesis, further functional studies are necessary.

Acknowledgment. The authors are grateful to Ursula Horr and John Moyers for processing the photographs. The help of Dr B. Ottenwälter and Dr A. Therani (Medigenomix GmbH, Planegg/Martinsried, Germany), Dr T. Kempf (Deutsches Krebsforschungszentrum, Heidelberg, Germany), Dr B. Kränzlin (ZMF, University of Heidelberg, Mannheim, Germany), Dr G. Heuschen (Department of Surgery, University of Heidelberg, Heidelberg, Germany), M. Keith, and C. Rohr is acknowledged with great appreciation.

REFERENCES

1. Gore RM: Small intestinal cancer. Clinical and pathological features. Radiol Clin North Am 35:351-356, 1997
2. Wheeler JMD, Warren BF, Mortensen NJ, et al: An insight into the genetic pathway of adenocarcinoma of the small intestine. Gut 50:218-223, 2002
3. Fearon ER, Vogelstein B: A genetic model for colorectal tumorigenesis. Cell 61:759-767, 1990
4. Yamashita Y, Kurnabe T, Cho YY, et al: Fatty acid induced glioma cell growth is mediated by the acyl-CoA synthetase 5 gene located on chromosome 10q25.1-q25.2, a region frequently deleted in malignant gliomas. Oncogene 19:5919-5925, 2000
5. Faergeman NJ, Knudsen J: Role of long-chain fatty acyl-CoA esters in the regulation of metabolism and in cell signalling. Biochem J 323:1-12, 1997
6. Black PN, Faergeman NJ, DiRusso CC: Long-chain acyl-CoA-dependent regulation of gene expression in bacteria, yeast and mammals. J Nutr 130:305S-309S, 2000
7. Black PN, DiRusso CC: Molecular and biochemical analysis of fatty acid transport, metabolism and gene regulation in *Escherichia coli*. Biochim Biophys Acta 1210:129-145, 1994
8. Van Aalten DMF, DiRusso CC, Knudsen J: The structural basis of acyl coenzyme A-dependent regulation of the transcription factor FadR. EMBO J 20:2041-2050, 2001
9. Shrago E: Long-chain acyl-CoA as a multi-effector ligand in cellular metabolism. J Nutr 120:290S-293S, 2000
10. Oikawa E, Iijima H, Suzuki T, et al: A novel acyl-CoA synthetase, ACS5, expressed in intestinal epithelial cells and proliferating preadipocytes. J Biochem (Tokyo) 124:679-685, 1998
11. Knudsen J, Neergaard TBF, Gaigg B, et al: Role of acyl-CoA binding protein in acyl-CoA metabolism and acyl-CoA-mediated cell signaling. J Nutr 130:294S-298S, 2000
12. Kitajka K, Puskás LG, Zvara Á, et al: The role of n-3 polyunsaturated fatty acids in brain: Modulation of rat brain gene expression by dietary n-3 fatty acids. Proc Natl Acad Sci USA 99:2619-2624, 2002
13. Puskás LG, Kitajka K, Nyakas C, et al: Short-term administration of omega 3 fatty acids from fish oil results in increased transthyretin transcription in old rat hippocampus. Proc Natl Acad Sci U S A 100:1580-1585, 2003
14. Kuhajda FP, Jenner K, Wood FD, et al: Fatty acid synthesis: A potential selective target for antineoplastic therapy. Proc Natl Acad Sci U S A 91:6379-6383, 1994

**This Page is Inserted by IFW Indexing and Scanning
Operations and is not part of the Official Record**

BEST AVAILABLE IMAGES

Defective images within this document are accurate representations of the original documents submitted by the applicant.

Defects in the images include but are not limited to the items checked:

- BLACK BORDERS**
- IMAGE CUT OFF AT TOP, BOTTOM OR SIDES**
- FADED TEXT OR DRAWING**
- BLURRED OR ILLEGIBLE TEXT OR DRAWING**
- SKEWED/SLANTED IMAGES**
- COLOR OR BLACK AND WHITE PHOTOGRAPHS**
- GRAY SCALE DOCUMENTS**
- LINES OR MARKS ON ORIGINAL DOCUMENT**
- REFERENCE(S) OR EXHIBIT(S) SUBMITTED ARE POOR QUALITY**
- OTHER: _____**

IMAGES ARE BEST AVAILABLE COPY.

As rescanning these documents will not correct the image problems checked, please do not report these problems to the IFW Image Problem Mailbox.